



Electrostatic Discharge and Electromagnetic Interference Design and Testing of Power Plant Safety Control Cabinet

A Major Qualifying Project Report

Submitted to the Faculty
of the

WORCESTER POLYTECHNIC INSTITUTE

in partial fulfillment of the requirements for the
Degree of Bachelor of Science
in Electrical and Computer Engineering
by

Jola Myrta

Approved by:

Professor Peder C. Pedersen

March 1, 2010

Table of Contents

Table of Contents	2
Table of Figures	4
Table of Tables	6
List of Equations	7
Acknowledgements	8
Abstract	9
1. Introduction	10
2. Background	12
2.1 Nuclear Industry	12
2.2 Standards	12
2.3 Pressure Water Reactor	13
2.4 Shin Kori 3 & 4 APR1400	15
3. Auxiliary Process Cabinet- Safety	17
3.1 Qualification Requirements	17
3.2 Equipment Safety Classification	18
3.3 Acceptance	19
3.3.1 Seismic	19
3.3.2 Environmental	19
3.4.3 Electromagnetic Compatibility	19
3.4.4 Fault	20
4. Test Procedure for Monitoring the Signal Conditioning	21
4.1 Modules	21
5. Electrostatic Discharge	24
5.1 Introduction	24
5.1.1 Human Body Model	25
5.1.2 Machine Model	26
5.1.3 Charged Device Model	27
5.2 Electrostatic Discharge of Signal Conditioning Modules	28
5.3 Design of Enclosure	28
5.3.1 Software Used	29
5.3.2 Machining	31
5.4 Software Analysis	31
5.4.1 Background of Electromagnetism	32
5.4.2 Testing and Analysis	35
5.4.3 Results	36
6. Results	55
6.1 Introduction	55
6.2 ESD Test Results	57
6.2.1 Modules	57
6.2.2 Aluminum Enclosure	58
6.2.3 Stainless Steel Enclosure	59
6.3 Compare Software and Testing Results	59
7. Conclusions	60

References.....	62
Appendix A: Standards.....	63
Appendix B: Wiring Diagrams For Each Module.....	64
Wiring description for the W5206.....	64
Wiring description for the W5207.....	65
Wiring description for the W5214.....	66
Wiring description for the W5229.....	67
Wiring description for the W5216.....	68
Wiring description for the W5218.....	69
Wiring description for the W5221.....	70
Wiring description for the W5224.....	71
Wiring description for the W5227.....	72
Wiring description for the W5228.....	73
Wiring description for the W5204.....	74
Wiring description for the W5202.....	75
Wiring description for the W5205.....	76
Appendix C: Test Equipment.....	77
Appendix D: Test Setup.....	78
Appendix E: Expected Outputs with Tolerances.....	80
Appendix F: Ideal Expected Outputs.....	82

Table of Figures

Figure 1 Artist Rendition of Shin Kori 3&4	17
Figure 2: Wiring of the Modules inside cabinet	22
Figure 3: Fluke Calibrators	22
Figure 4: Output to the Datalogger	22
Figure 5: Wiring diagram from terminal blocks to input and output module.....	23
Figure 6: Typical Human Body Model Circuit.....	25
Figure 7: Worst Case, Actual Human Body Model Circuit.....	26
Figure 9: Machine Model Circuit	26
Figure 10: Charged Device Model.....	27
Figure 11: Dimensions of Module Make	29
Figure 12: Sheet metal Design.....	30
Figure 13: Top Sheet Metal Design	30
Figure 14: Enclosure with Module	31
Figure 15: Global Setup.....	35
Figure 16: Aluminum Impressed x E-Field	36
Figure 17: Arrows of electric field strength.....	37
Figure 19: Values for chosen point on surface	38
Figure 18: Chosen value on surface.....	38
Figure 20: Graph of front.....	39
Figure 21: Aluminum Impressed y E-field	39
Figure 22: Arrows of electric field strength.....	40
Figure 24: Values from chosen point on surface	41
Figure 23: Chosen value on surface.....	41
Figure 25: Graph of Front	42
Figure 26: Aluminum Impressed z E-field	42
Figure 27: Arrows of electric field strength.....	43
Figure 28: Chosen value on surface.....	44
Figure 29: Values from chosen point on surface	44
Figure 30: Graph of front.....	45
Figure 31: Stainless Impressed x E-field	45
Figure 33: Chosen value on surface.....	46
Figure 32: Arrows of electric field strength.....	46
Figure 34: Values from chosen point on surface	47
Figure 35: Graph of front.....	47
Figure 36: Stainless Impressed y E-field	48
Figure 37: Arrows of electric field strength.....	48
Figure 39: Values from chosen point on surface	49
Figure 38: Chosen value on surface.....	49
Figure 40: Graph of front.....	50
Figure 41: Arrows of electric field strength.....	51
Figure 43: Values from chosen point on surface	52
Figure 42: Chosen value on surface.....	52
Figure 44: Graph of front.....	53
Figure 46: Set-up of test bench	56

Figure 45: Test Levels	56
Figure 47: Data Logger Software	57
Figure 48 Wiring diagram for the W5206	64
Figure 49 Wiring diagram for the W5207	65
Figure 50 Wiring diagram for the W5207	66
Figure 51 Wiring diagram for the W5229	67
Figure 52 Wiring diagram for the W5216	68
Figure 53 Wiring diagram for the W5218	69
Figure 54 Wiring diagram for the W5221	70
Figure 55 Wiring diagram for the W5224	71
Figure 56 Wiring diagram for the W5227	72
Figure 57 Wiring diagram for the W5228	73
Figure 58 Wiring diagram for the W5204	74
Figure 59 Wiring diagram for the W5202	75
Figure 60 Wiring diagram for the W5205	76

Table of Tables

Table 1: Electric Field Strength of Aluminum and Stainless Steel	53
Table 2: Results for Aluminum.....	58
Table 3: Results for Stainless Steel.....	59

List of Equations

Equation 1: Output Calculation for the W5206 Module.....	82
Equation 2: Output Calculation for the W5207 Module.....	82
Equation 3: Output Calculation for the W5214 Module.....	83
Equation 4: Output Calculation for the W5229 Module.....	83
Equation 5: Output Calculation for the W5216 Module.....	84
Equation 6: Output Calculation for the W5218 Module.....	84
Equation 7: Output Calculation for the W5221 Module.....	85
Equation 8: Output Calculation for the W5224 Module.....	85
Equation 9: Output Calculation for the W5227 Module.....	86
Equation 10: Output Calculation for the W5228 Module.....	86
Equation 11: Output Calculation for the W5204 Module.....	87
Equation 12: Output Calculation for the W5202 Module.....	87
Equation 13: Output Calculation for the W5205 Module.....	88

Acknowledgements

I would like to thank Professor Peder Pedersen for advising this project. I would like to acknowledge Westinghouse Electric Company, for their funding and opportunity to allow WPI to be a part of their cutting edge research and development. I also offer gratitude to Westinghouse Nuclear Company for the travel and testing experience conducted in New Stanton, PA. I would like to acknowledge Integrated Software for their COULOMB3D electric field solver software.

Abstract

This project conducts an innovative approach to prevent electromagnetic interference and electrostatic discharge affecting the Auxiliary Process Safety Cabinet (APC-S) in the South Korean Nuclear Power Plant 3 and 4, also known as Shin Kori 3 &4. The Auxiliary Process Safety Cabinet consists of the Acromag Signal Conditioners and is required to function and maintain structural integrity before, during and after all tests. Research was conducted on the causes and how to prevent electrostatic discharge from damaging electric components. As the signal conditioners were provided from a manufacturer the design of the components could not be changed. The solution was to design a metal enclosure to protect the inside components from any electrostatic discharge. The modules needed to be accessible in the enclosure in case of any failure. This then lead to the idea of having an enclosure that consisted of two parts. By designing a metal enclosure for the Acromag signal conditioner modules it was proven that they passed Electrostatic Discharge testing. This was shown by conducting both software analysis and testing on aluminum and stainless steel enclosures.

1. Introduction

This project conducts an innovative approach to prevent electromagnetic interference and electrostatic discharge affecting the Auxiliary Process Safety Cabinet (APC-S) in the South Korean Nuclear Power Plant 3 and 4, also known as Shin Kori 3 &4. The APC-S cabinet will be tested for Seismic, Electromagnetic, Environmental and Electrostatic Discharge. This project will focus on the design and testing for electrostatic discharge. The cabinet is required to function and maintain structural integrity before, during and after all tests.

This project will consist of the design of the Auxiliary Process Cabinet- Safety and an enclosure design of the Acromag modules to be protected from Electrostatic discharge. The design of the APC-S consists of 13 Acromag signal conditioner modules that receive signals from different sensors throughout the plant and split the signals to a safety and non-safety system. It is important for these modules to maintain their functionality so that these two systems do not communicate with one another.

Engineering activities in this project has included the design of the final wiring diagram, the drawings of the test set up as it is placed in the cabinet, and the set up of all modules and mount into cabinet connect both the input and output. The final wiring diagram was determined after the functions of the 13 modules were studied. In the drawing the input of the module is shown and the output that is connected to the data logger. The design of an aluminum and stainless steel enclosures was important to protect the modules from high voltages, electrostatic discharge. The modules were only tested at medium level. Numerical software that will predict the field distribution for the enclosure in orthogonal directions was conducted using COULOMB software.

The software was important to predict if the modules would pass. The modules were then manufactured after being designed in SolidWorks at the machine shop at Worcester Polytechnic Institute. After the modules enclosures were completed they were sent down to complete experimental testing that was conducted in New Stanton, PA by Washington Labs Facility. The data collected from testing of the modules was then compared to the experimental results of COULOMB.

The output data was recorded using the FLUKE 2640/2645 NetDAQ Data Logger. This data logger will read all of the output results every 1/10 seconds. The software that was used to run analytical field distributions is Integrated Software COULOMB.7. COULOMB.7 provides many features such as analysis of electrical conduction and loss dielectrics, simulation of non-linear conductivity and permittivity, and ability to assign constant or non-uniform charge distributions to surfaces, as well as many other features.

In the second chapter background of the nuclear industry and the design of this nuclear power plant, Shin Kori 3 & 4 is presented. In the third chapter the Auxiliary Process Cabinet is introduced and the tests that are being conducted. In the fourth chapter the modules and their functions are explained. In the fifth chapter electrostatic discharge research is shown and the how it will affect the modules. Lastly in chapter six the results for software analysis and experimental testing are compared.

2. Background

2.1 Nuclear Industry

The nuclear industry began with the Manhattan Project of World War II, which ended in the making of the first atomic bombs. After the war ways were sought to bring peaceful and commercial uses to this new technology. In the early 1950s, a bill was signed into creating the Atomic Energy Commission with the purpose to promote and control the use of the atom. As technology grew the laws and regulations changed to reflect the knowledge learned and establish limits for construction and operation.

In 1954 the Nuclear Regulatory Commission was formed to oversee, set rules and standards for the commercial use of nuclear materials. The Atomic Energy Commission were not only regulating the industry but also promoting it. In the 1970s the commission stopped promoting nuclear power but continues to regulate the industry due to Three Mile Island. The Nuclear Regulatory Commission consists of five commissioners one of which is named Chairman by the United States of America. The NRC protects the health and safety of the general public.

2.2 Standards

Agencies in charge of providing guidelines of the nuclear power industry are American National Standards Institute (ANSI), American Society of Mechanical Engineers (ASME), Institute of Nuclear Power Operations (INPO), International Commission on Radiological Protection (ICRP), International Commission on Radiation Units (ICRU), National Council on Radiation Protection and Measurement (NCRP), Institute of Electrical and Electronics Engineers (IEEE) and more.

The ASME provides guidelines and standards on piping, valves and mechanical systems. INPO was formed to provide an independent group which sets standards of excellence. ICRP and ICRU have set radiation standards on international level while NCRP has done the same thing in the United States. The purpose of the agencies is to provide standards, limits, and guidelines which protect the public and workers and still provide freedom for the economical incentive for nuclear power.

2.3 Pressure Water Reactor

A pressurized water reactor system utilizes two separate heat transfer loops to accomplish the production of steam for turbine-generator operation. These heat transfer loops are referred to as the primary system and the secondary system. The primary loop consists of the reactor vessel, reactor coolant pumps, pressurizer, steam generator tubes and interconnecting piping. The secondary system consists of the shell side of the steam generators; high and low pressure turbines, moisture/separator re-heaters, main electrical generator, main condenser, condensate and feed pumps, and interconnecting piping.

Pressurized water reactor defines the coolant to be used as the heat transfer medium, and describes the conditions at which the coolant will exist. The coolant used is light water which is pressurized at approximately 2250psi. The coolant is pressurized so that its temperature can be raised above the boiling point of 212°F allowing for the production of steam in the secondary side of the steam generator.

In operation, the uranium fuel in the reactor vessel produces large amounts of heat during the fission process. The reactant coolant flows past the fuel in the channels in the core and absorbs

the heat being produced. The coolant is then pumped through the tubes in the steam generator where this excess heat is transferred to the feedwater surrounding these tubes. This heat transfer causes the feedwater to boil, producing steam in the secondary side of the steam generator. A large storage vessel is connected to the loop to absorb changes in the coolant volume and to maintain system pressure at the required 2250psi. The reactant coolant system is maintained in a sub cooled liquid state to prevent possible fuel or system damage. The temperature-pressure relationship of the coolant should be maintained within a normal range to prevent bulk boiling.

In the secondary system, the steam produced by the boiling of feedwater is directed to high and low pressure turbines which are coupled to an electrical generator. The steam is used to rotate the high and low pressure turbines which causes condensed in the main condensers and this condensate is pumped to the feed pump suction. The feed pump raises the pressure of the feedwater and pumps it back into the steam generator to repeat the cycle.

2.4 Shin Kori 3 & 4 APR1400

This section explains on how the Shin Kori power plant will run and how much power it will produce. Although this project is a small part of a power plant every single component needs to be operating at the exact specification for it this plant to properly produce power. The APR1400 is an evolutionary advanced light water reactor based on the Westinghouse Combustion Engineering (CE) System 80+ technology. The 80+ standard plant design is a 1300 MWe¹ pressurized water reactor based on evolutionary improvements to the standard CE System 80 nuclear steam supply system and a balance-of-plant design developed by Duke Power Co. The System 80+ design has safety systems that provide emergency core cooling, feedwater and decay heat removal. It also contains a safety depressurization system for the reactor, a combustion turbine as an alternate AC power source, and an in-containment refueling water storage tank to enhance the safety and reliability of the reactor system.

The nuclear steam supply system of the APR1400 is rated at 4,000 MWt² with a net electrical generation of 1,400 MWe. The Korean Nuclear Industry decided to standardize its advanced reactor design based on this technology in the mid-1990s and spent the next 10 years developing the detailed design. Westinghouse participated in this design effort under the Korean Next Generation Reactor (KNGR) contract executed from 1997 through 2000. This partnership eventually translated into signing of the SKN 3&4 contract in September 2006.

The scope for the two units consists of component design, equipment supply, project management, and consulting services. Major mechanical equipment supplied under the contract

¹ Megawatt Electric which refers to electric power

² Megawatt Thermal which refers to thermal power produced

consists of equipment manufactured at Nuclear Components Manufacturing, including one set of reactor vessel internals; eight reactor coolant pumps; one set of control element drive mechanisms and associated tooling; and control element assemblies, manufactured by Westinghouse Nuclear Fuel. Also supplied were reactor coolant pump motors, reed switch position indicators, the boronometer, and the process radiation monitor, all purchased from outside vendors. In addition to the mechanical equipment, Westinghouse will supply an integrated I&C architecture for both the Nuclear Steam Supply System (NSSS) I&C and the balance-of-plant systems and control facilities, which is a major difference between Shin Kori 3 and 4 and previous Korean Standard Nuclear Plants. The NSSS I&C includes the protection systems and NSSS-related control and monitoring. The balance-of-plant I&C includes systems for safety and non-safety component control, man-machine interfaces, and the control-room facilities.

Shin Kori 3&4 will be the thirteenth and the fourteenth nuclear units in the Republic of South Korea based on Westinghouse CE technology, as well as the nineteenth and twentieth overall based on Westinghouse technology. Shin Kori consists of 6 units total, 1&2, 3&4 and 5&6. Currently, Shin Kori 1 &2 are under construction.



Figure 1 Artist Rendition of Shin Kori 3&4

3. Auxiliary Process Cabinet- Safety

The Auxiliary Process Cabinet for Safety and Non-Safety houses analog signal conditioning and splitting electronics for the Reactor Coolant Pump Speed Sensors and conventional field instrumentation. The signal conditioners and splitters receive signals from various field sensors which condition and split, transmitting the output signal to different system such as the safety and non safety, and cabinets throughout the Nuclear Power Plant.

3.1 Qualification Requirements

The purpose of qualification requirements is to identify the equipment qualification actions required to be performed by the Signal Conditioning Instrumentation equipment supplier for the Shin-Kori Units 3 and 4 nuclear power plants and that requirements are met. The signal conditioning components are planned to be used in the Safety System Cabinets of the Auxiliary Process Cabinet-Safety (APC-S), Core Protection Calculator System (CPCS), Qualification and Indication Alarm System- PAMI (QIAS-P), and the Engineered Safety Feature- Component Control System (ESF-CCS) Group Controllers and Loop Controllers.

This specification defines the seismic, environmental, Electromagnetic Compatibility (EMC), and fault isolation test conditions, specific qualification requirements and methods to be employed in the performance of the qualification activities. The equipment shall meet the required performance requirements during seismic, environmental, EMC, and fault isolation testing.

The Safety System Cabinets in which the signal conditioning equipment will be installed are required to be qualified as Seismic Category I. The signal conditioning equipment is required to function and maintain structural integrity during and after design basis event conditions.

3.2 Equipment Safety Classification

The highest classification of the safety-related signal conditioning equipment planned to be used for SK3&4 is Class 1E, Seismic Category I. Class 1E (Safety) Seismic Category I equipment is required to function and maintain structural integrity before, during and after a *Safe Shutdown Earthquake* (SSE) seismic event. Non-safety related equipment whose continued function is not required but whose failure could impact proper functioning of adjacent safety-related Seismic Category I equipment is defined as

Non-Safety, Seismic Category II. Non-Safety, Seismic Category II equipment must maintain structural integrity during and after the SSE. The signal conditioning equipment planned to be used in SK3&4 will be used in both Class 1E (Safety) Seismic Category I and Non-Safety Category II applications.

3.3 Acceptance

Qualification activities performed shall demonstrate the signal conditioning equipment meets the seismic, environmental, EMC, and fault isolation requirements.

3.3.1 Seismic

Seismic qualification performed shall demonstrate that the Seismic Category I Signal Conditioning Equipment will maintain structural integrity during and after an earthquake at the SSE level preceded by the equivalent of five earthquake simulations at the one-half SSE level. Signal Conditioning Equipment is required to demonstrate it can perform its designated safety related functions before, during, and after each seismic test.

3.3.2 Environmental

Environmental qualification performed shall demonstrate the signal conditioning equipment continues to perform its designated safety related functions when subjected to the temperature and humidity conditions contained within this specification. Additionally, a qualified life for the Class 1E signal conditioning equipment shall be determined in accordance with the requirements of IEEE-323-1983 as noted by Regulatory Guide 1.89.

3.4.3 Electromagnetic Compatibility

Electromagnetic Compatibility testing shall be performed to demonstrate the signal conditioning equipment continues to perform its designated safety-related functions during and after continuous and transient EMC events. The signal conditioning equipment shall be designed to lower the susceptibility to externally generated EMI/RFI and power surges. The Supplier shall

also design the system to minimize the generation of EMI/RFI, thus becoming a potential source of interference as described in WNA-DS01220-SHIN-K3 (Reference 1).

3.4.4 Fault

Fault testing shall be performed to demonstrate isolation devices meet the criteria. The isolation devices shall be monitored and recorded during the fault test signal to demonstrate physical independence of the electrical circuits. Testing shall be conducted in both the common mode configuration (i.e., between output signal supply terminal and ground, then between output signal return terminal and ground) and the transverse mode configuration (between output signal supply and return terminals).

4. Test Procedure for Monitoring the Signal Conditioning

Test guidelines and/or monitoring procedures for the Acromag Signal Conditioning modules that will be used in the Auxiliary Process Safety Cabinet. This document identifies all of the test equipment needed to test the modules. Monitoring instructions for EMI testing and a recommended test report format are also detailed in this document.

4.1 Modules

The Signal Conditional modules test plan and monitoring procedures are detailed in this MQP Report. The test set up, monitoring procedure and expected output values can be found in Appendix C, D, and E. Each module is to be tested according to procedures specified in this document. Modules W5218, W5221, W5224, W5227, and W5228 are Resistance Temperature Detector (RTD). Modules, W5207, W5214, and W5229 are thermocouples. Module W5206 is a voltage to current converter, module W5216 is a potentiometer/slide wire to current converter, modules W5204, W5205 are current to current isolators, and module W5202 is a current to voltage isolator. The wiring diagrams for each of the modules can be found in Appendix B. The final wiring diagram is shown in Figure 5, which shows the modules that are connected through terminal blocks and the input and output signals. The thermocouple and RTD simulator were inputs provided by Fluke Calibrators shown in Figure 3. The output wires are connected directly into the data logger card which can be seen below in Figure 4. A wiring diagram was constructed by me and a fellow engineer, a drawing of which is shown in Figure 5.

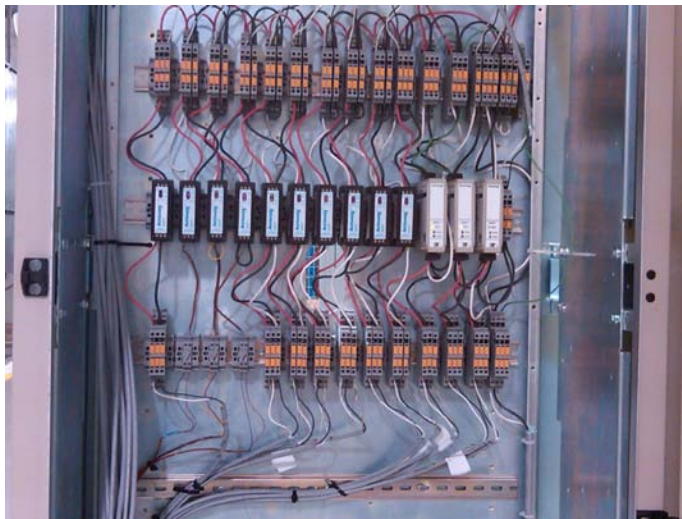


Figure 2: Wiring of the Modules inside cabinet



Figure 3: Fluke Calibrators

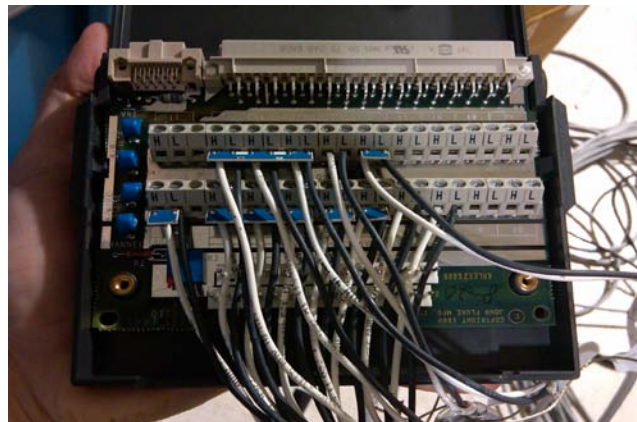


Figure 4: Output to the Datalogger

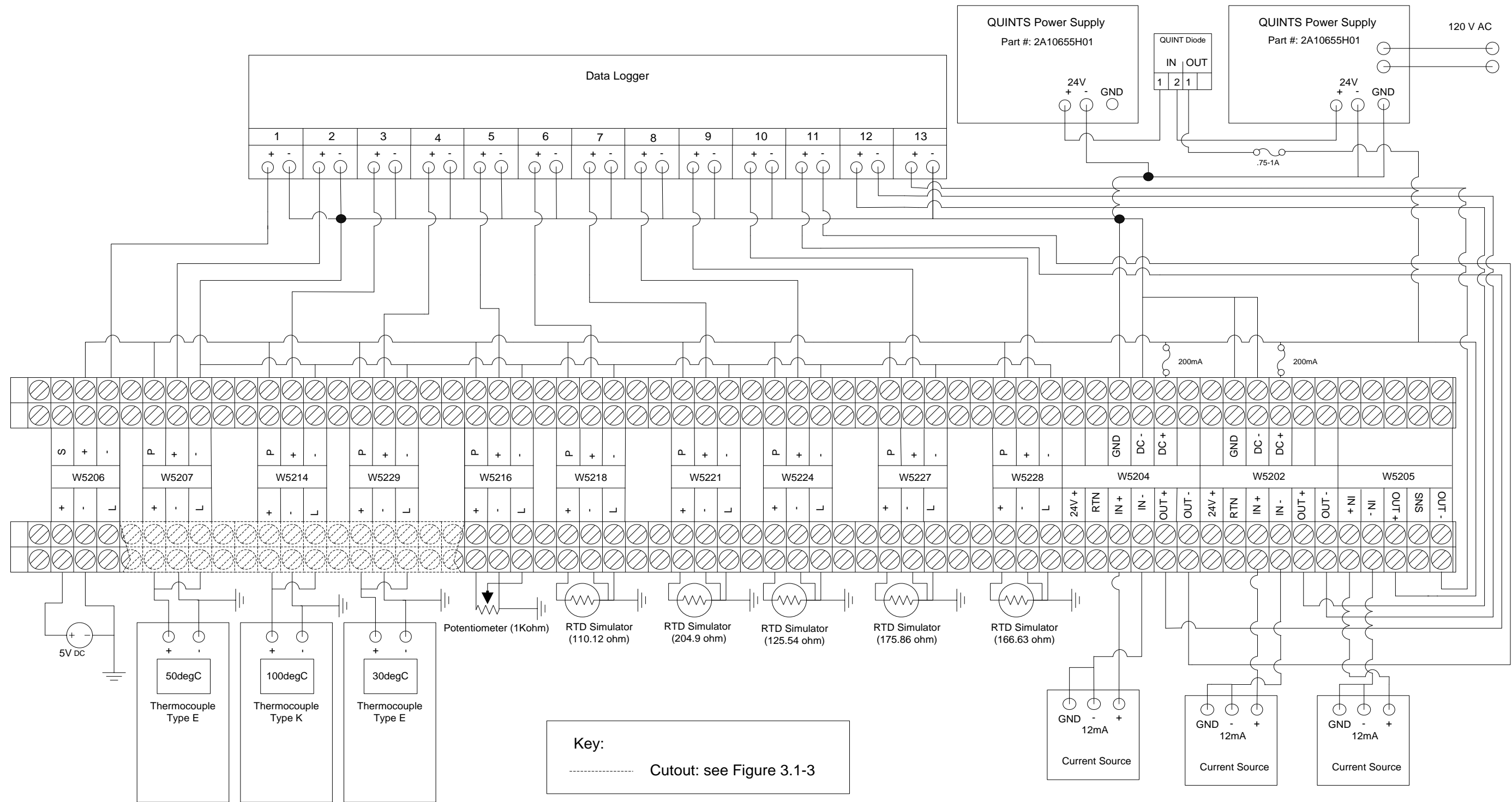


Figure 5: Wiring diagram from terminal blocks to input and output module

5. Electrostatic Discharge

5.1 Introduction

Static electricity is an electrical charge caused by an imbalance of electrons on a given a surface of material. Electrostatic discharge is the transfer of electric charge between bodies of different electrostatic potential in proximity or through direct contact. When electric charge is transferred between two materials, the one that loses electrons becomes positively charged and the one that gains electrons is negatively charged. The damages caused by electrostatic discharge can change the electrical characteristics of a device and how it functions.

Static electricity is measured in Coulombs and represented by the symbol Q . The charge “ Q ” is equal to the capacitance times the voltage potential of the object. When testing for the static electricity the amount of voltage being applied and a rough capacitance is given to us and we are able to solve for the charge which can be positive or negative.

The material chosen for the enclosure is either Aluminum Alloy 1100 or Stainless Steel, both of which are conductive materials and have low electrical resistance which allows electrons to flow through a given surface very easily. If a conductor, such as aluminum, is connected to an earth ground point all of the electrons will flow to ground and any excess charges will be neutralized, protecting any electrical component inside of the enclosure from contact.

5.1.1 Human Body Model

The Human Body Model is the most common model that causes electrostatic discharge damage. If a person walks across a floor, an electrostatic charge accumulates on the body. A person has an effective capacitance up to of 300 picofarads. A device is contacted by hand, and this allows the body to discharge which can lead to a failure to the device. The required human body model immunity levels typically range between 1kV to 8kV. The typical human body model circuit is represented in Figure 6. The worst case human body model is represented in Figure 7, where the charge resistance, R_{charge} is usually 1 M ohm, the body capacitance, C_{body} ranges between 60 to 300 picofarads, the body resistance ranges between 150 to 1500 ohms. The hand capacitance ranges between 3 to 10 picofarads and the hand resistance ranges between 20 to 200 ohms.

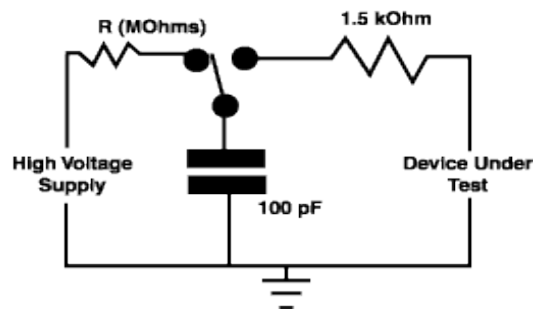


Figure 6: Typical Human Body Model Circuit³

³ Fundamentals of Electrostatic Discharge, Electrostatic Discharge Association (Electrostatic Discharge Association, 2001) <http://www.esda.org/basics/part1.cfm>

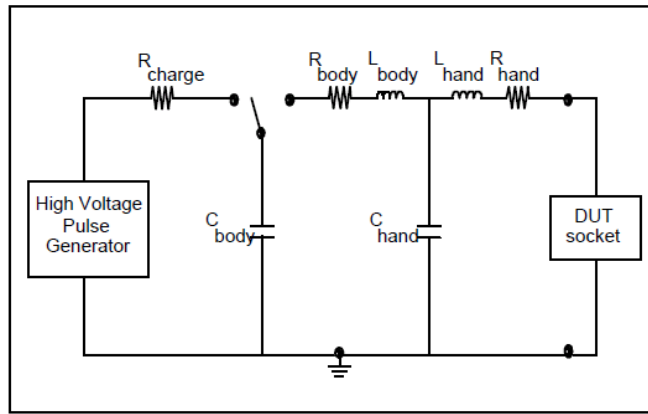


Figure 7: Worst Case, Actual Human Body Model Circuit

Typical Voltage Levels at Different Relative Humidities		
Means of Generation	0—25% RH	65—90% RH
Walking across carpet	35,000 V	1500 V
Walking across vinyl tile	12,000 V	250 V
Worker at bench	6000 V	100 V
Poly bag picked up from bench	20,000 V	1200 V
Chair with urethane foam	18,000 V	1500 V

Figure 8: Voltages⁴

5.1.2 Machine Model

The Machine Model simulates a more rapid and severe electrostatic discharge from a machine, fixture, or tool that may be charged. It is when a machine becomes electrostatically charged from a manufacturing facility and discharges into a circuit when contacted. This is modeled by a charged capacitor and an inductive discharge, which indicates the characteristics of a machine rather than a human.

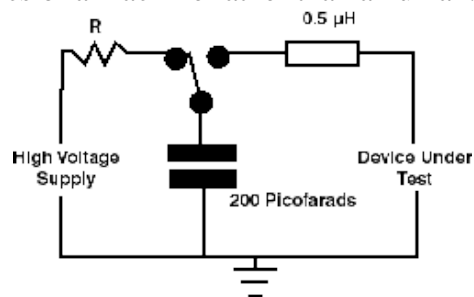


Figure 8: Machine Model Circuit⁵

⁴ (Electrostatic Discharge Association, 1999)

⁵ (Electrostatic Discharge Association, 2001)

5.1.3 Charged Device Model

The Charged Device Model test method takes the place of the Machine Model testing for ESD. This method shows what happens in an automated manufacturing environment when an IC (Integrated Circuit) becomes triboelectrically (static charge due to rubbing) charged, and the part discharges when it comes in contact with a grounded conductor. Integrated Circuit is what is known as a chip, where all of the electric components are manufactured in small surface of a semiconductor material. The triboelectric effect is manifested when a material becomes electrically charged after rubbing against a different material. Depending on the materials that come into contact with one another, the polarity and strength of the charges differ depending on the material. This is a more challenging device to model, and is based on the size and the capacitance of the IC being tested, with little impedance to reduce the current. This can result in high currents, 5A to 6A being discharged in a short duration of one nanosecond or less. The charged model is shown in Figure 10.

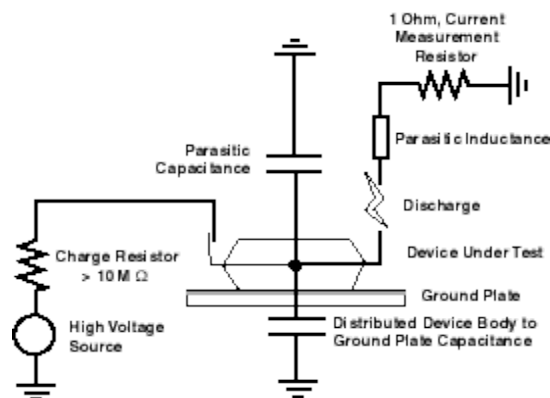


Figure 9: Charged Device Model⁶

⁶ (Electrostatic Discharge Association, 2001)

There are two main purposes for the three ESD testing of an integrated circuit. The first is to determine ESD immunity of the IC, which ensures that the product can be confidently used in a Nuclear Power Plant, where safety and reliability are most important. The second purpose is to identify what the failure mechanisms are on the devices that are being tested. ESD testing is ultimately a destructive test, so testing requires multiple tries.

5.2 Electrostatic Discharge of Signal Conditioning Modules

The APC-S consists of thirteen (13) signal conditioning modules that are qualified for electrostatic discharge at 4kV contact discharge and 8kV air discharge. The APC-S will be tested at 8kV contact discharge and 15kV air discharge. In order to be confident that these modules would pass, plan B was to design an aluminum and stainless steel enclosure that will be connected to ground. Plan A was testing the modules as is without any enclosure. It was decided that an enclosure would need to be designed since the modules were only guaranteed that they would pass up to 4kV contact and 8kV air discharge.

5.3 Design of Enclosure

Before designing the enclosure the dimensions were measured and compared to the dimensions given in the data sheet. Each module has three input and three output wires, a din-rail mounting which is clipped to the cabinet, and a span switch. These openings had to be designed on the enclosure. In Figure 11 the dimensions and openings of the module are given.

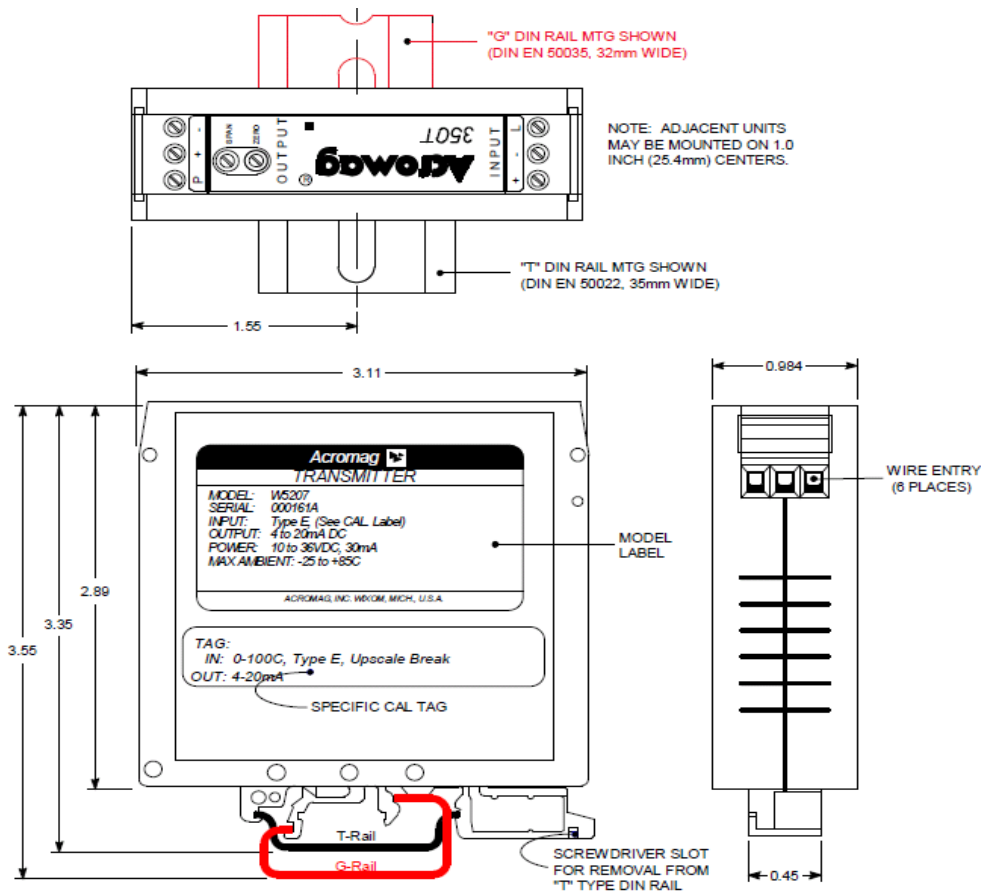


Figure 10: Dimensions of Module Make⁷

5.3.1 Software Used

The enclosure was designed using a computer aided design program, SolidWorks2009. In SolidWorks the sheet metal design was chosen to construct the enclosure. The main concern of the design was that the module needed to be accessible in minutes in case of failure. The constraining parameters were the openings that needed to feed the wire to connect to the input and output signals, and the bottom of the module needed to be open in order for din rail mounting to connect into the cabinet yet keep the module secure in the enclosure. The sheet metal is shown in Figure 12 with the respective openings. The second part of the enclosure is the top part with a small flap to keep the module from dispensing. The two parts of the enclosure are shown in Figure 13. After the openings were made on

⁷ (Acromag Incorporated, 1993)

the sheet metal, three bends were made to complete the box look. The second part of the enclosure was bent at the bottom corner to secure the module inside. In Figure 14 the module is shown with the enclosure.

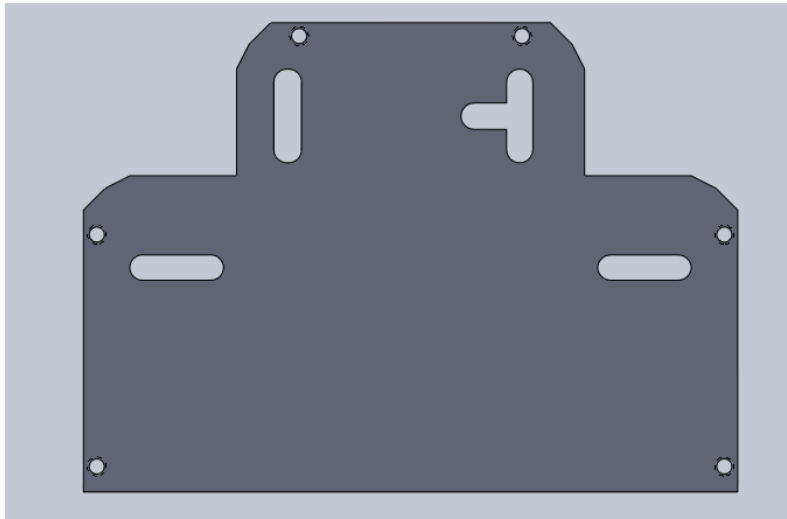


Figure 11: Sheet metal Design

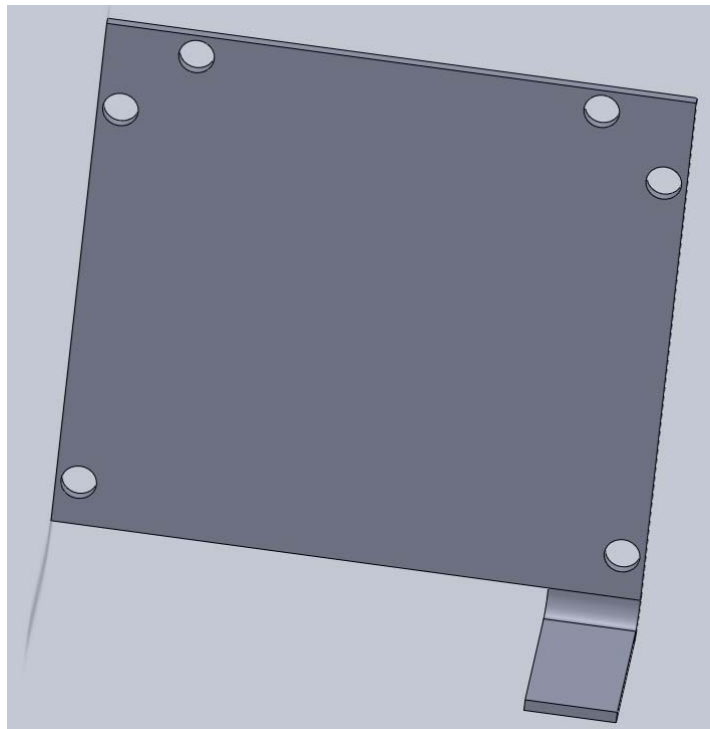


Figure 12: Top Sheet Metal Design

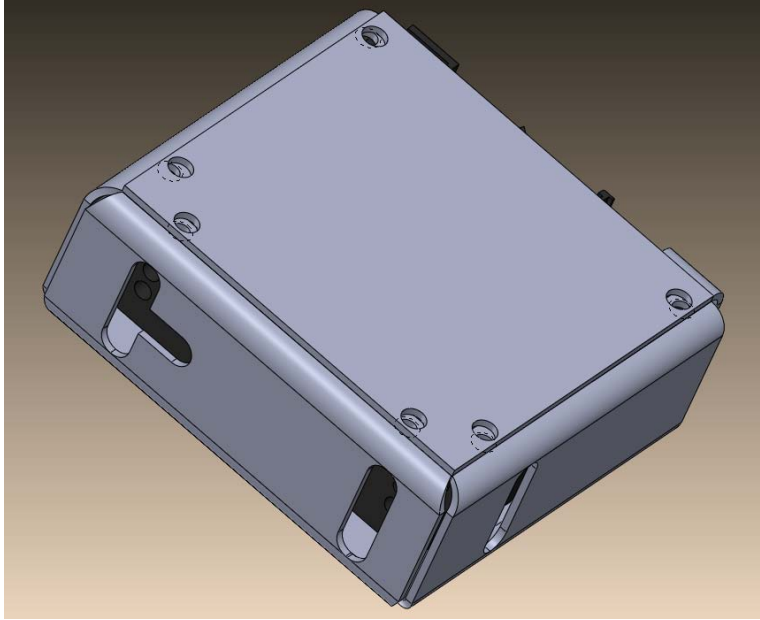


Figure 13: Enclosure with Module

5.3.2 Machining

After the design was completed in SolidWorks it was then imported into ESPRIT, which is a high-performance, full spectrum, and computer aided manufacturing system of machine tool applications. ESPRIT is then set up with VF3 milling machine in which the openings were machined. The machining was completed in WPI's Washburn Machine Shop. After the openings were completed the sheet metal was then taken to Higgins Machine Shop where the sheet metal was bent into a desired box shape and the second piece was attached.

5.4 Software Analysis

COULOMB 07

COULOMB is a software package designed to solve for the 3D low frequency electric field. COULOMB was provided by Integrated Software, located in Winnipeg, Manitoba, CANANDA. This 3D electric field design and analysis software features Boundary

Element Method and Finite Element Method. The Boundary Element Method is suited for applications where the design requires large open field analysis and exact model of boundaries. The Finite Element Method allows the selection of a suitable solver according to the application and verifies the results within the program. Some applications COULOMB is used for are: insulators, grounding electrodes, micro electro mechanical systems, high voltage shields, power transmission lines, and much more. To perform simulations using COULOMB the first requirement is to construct a geometric model of the physical system. This can be done in other software and imported into COULOMB, such as SOLIDWORKS. After the geometric model has been built, the physical properties are assigned (boundary conditions, materials, sources, etc.)

COULOMB allows users to enter custom material data information. The aluminum used to design the enclosure was Aluminum Alloy 1100, where the physical properties of this alloy does not differ much of from the standard aluminum but for more accurate results the changes were made. The physical properties for the stainless steel were also altered.

5.4.1 Background of Electromagnetism

As we are told in the first few years of undergraduate studies that theory is most important and in order to apply it to design courses and projects it has to be mastered. The theory of electromagnetism defines the phenomenon that occurs but not able to see. The materials that were chosen depended on their conductivity and permittivity values, which is expressed one of the formulas below. For any given material it is known that it consists of atoms, molecules, or ions. Within aluminum there exist electrons that are bound to

individual atoms or are free. When applying an electric field, the electrons will move due to the field. The electric current density is given below, which measures the flow of electrons and it varies with the strength of the electric field.

$$\bar{J}_c = \sigma_s \bar{E}$$

The constant σ_s is the conductivity, which provides the measure of how fast an electron can flow through a material, also known as the ability to conduct an electric current. The formula is defined below:

$$\sigma_s = -q\mu_e$$

Here q is the charge and μ_e is the electric mobility. The electric flux density varies linearly with the application of the electric field,

$$\bar{D} = \epsilon \bar{E}$$

The constant ϵ is the permittivity, which is a measure of how an electric field can affect a dielectric. It relates to a materials ability to transmit an electric field. Maxwell's Equations states that \bar{J} is the electric current density and it contains two parts. The first is the impressed electric current is \bar{J}_e , an input to the system by an outside source. The second is the conduction electric current density, \bar{J}_c caused by an external electric field.

$$\nabla \times \bar{H} = \bar{J}_e + \bar{J}_c + j\omega \bar{D}$$

$$\nabla \times \bar{H} = \bar{J}_e + \sigma_s \bar{E} + j\omega \bar{D}$$

This then leads to electric dipoles and at least one exists in most materials. An electric dipole is the separation of positive and negative charges. The three types of dipoles are.

1. Molecules arranged in a way to exhibit an imbalance of charge.
2. Ions have oppositely charged parts,

3. Most atoms have electrons surrounding the nucleus, thus causing the electrons to react and move quicker than the nucleus can react, when an electric field is applied.

When an external electric field is applied the dipoles align with the field, causing an extra term to be included in the electric flux density that contains the same vector direction as the applied field.

$$\bar{D} = \epsilon_0 \epsilon_r \epsilon \bar{E}$$

As the dipole adjusts to align with the field, in time the electric field will reverse its direction and the dipole moves with the field to remain in the correct polarity. The effective conductivity for a metal is due to the collision of electrons thus reducing Maxwell's Equation.

$$\nabla \times \bar{H} = \bar{J}_i + (j\omega\epsilon_0 + \sigma_s)\bar{E}$$

5.4.2 Testing and Analysis

The software analysis of COULOMB was performed on the aluminum and stainless steel enclosures. The model of the enclosure was designed in SolidWorks and then imported into COULOMB. After the geometric model was imported into COULOMB the physical properties were set. The outside material was assigned to either aluminum or stainless steel and the inside of the enclosure was assigned to air. In the Physical Global Setup menu shown in Figure 14, the solver type was set to fields so it was able to plot fields and analyze a force on a volume, the operation was set to static where all voltages are assigned at magnitude, and the material default is set to permittivity mode because the real part of the dielectric material is much smaller than the imaginary part and when there is no voltage drop applies to a material. Aluminum and stainless steel are both conductive materials and that is why the material is much smaller than the imaginary part.

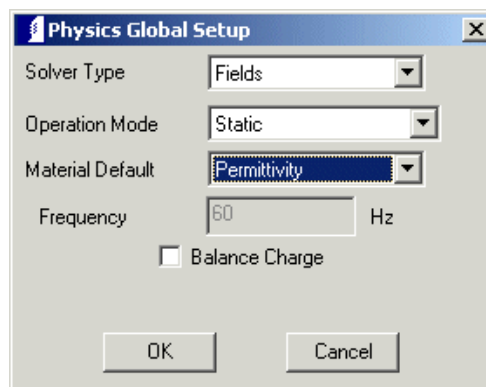


Figure 14: Global Setup

The next value assigned was the floating boundary on the surface of the conductors that do not have an assigned voltage, thus the surface “floats” to a constant value.

The surface charge creates the effect of trapped charge on a surface; this value depends on the physical phenomenon that occurs. The physical phenomenon that occurs is electrostatic

discharge which can be caused by human discharge, as mentioned in the section above.

The surface charge was set to 15,000V because it's the highest value that the modules were being tested for air-discharge. Once the charge is set an impressed field is assigned for x, y and z components.

5.4.3 Results

The test solver in COULOMB was utilized for the aluminum and stainless steel designed enclosures. The enclosures were tested in x, y, and z direction to compare the electric field strengths at a chosen point of a given surface. The modules were only tested from the front view of the enclosure since it's how they are mounted in the cabinet. The analysis that was conducted using COULOMB also compares the electric field strength of the front view.

The impressed field of the aluminum enclosure is shown in Figure 16 with the arrows facing in the upwards direction.

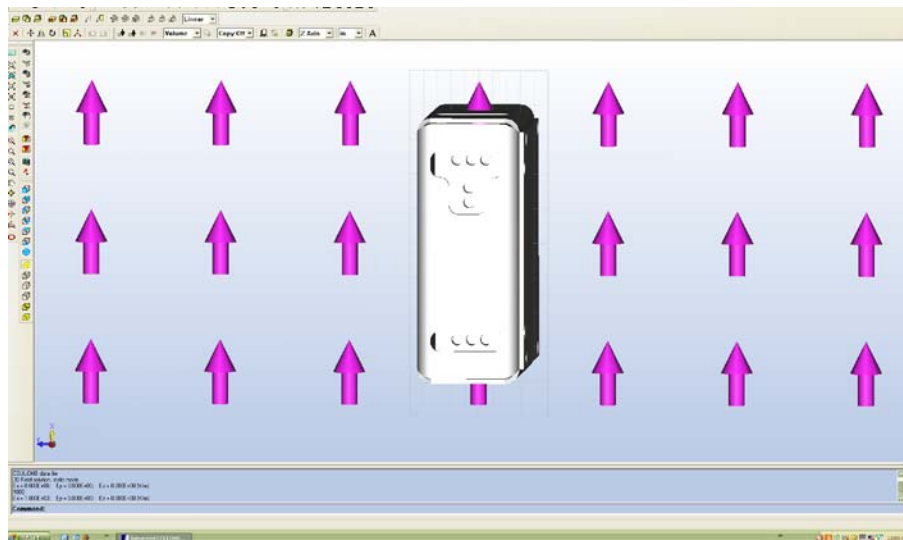


Figure 15: Aluminum Impressed x E-Field

In Figure 17 the arrows are shown to express the electric field strengths at the front of the enclosure. The arrow colors range from blue to red, blue being the lowest electric field strength and red being the highest.

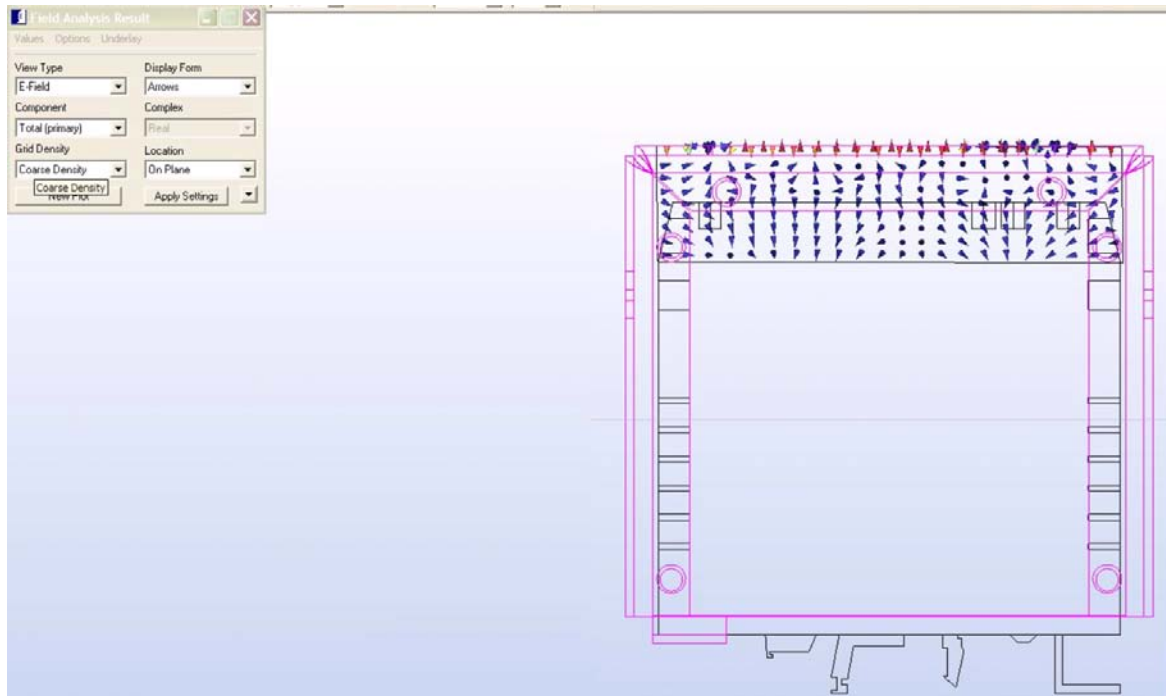


Figure 16: Arrows of electric field strength

In Figure 18 the field analysis result is solving for the electric field at a point on any surface. The values shown at the bottom of the screen display the electric field in the x, y and z directions and the magnitude.

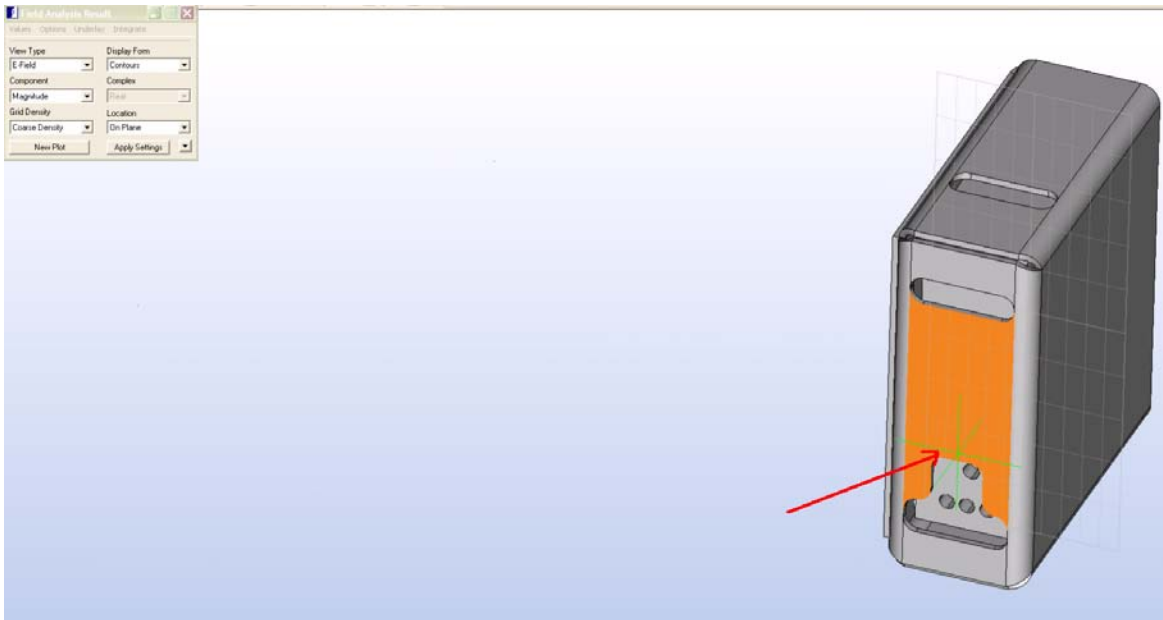


Figure 17: Chosen value on surface

The green point on the surface shows the values of the electric field that are in Figure 19 below.

Analysis completed at 11:15:28 on 12/21/09						
x(in)	y(in)	z(in)	Ex(V/m)	Ey(V/m)	Ez(V/m)	Em(V/m)
-1.445E+00	2.521E-01	1.930E+00	-5.499E+14	4.725E+13	5.317E+16	5.318E+16
x(in)	y(in)	z(in)	Ex(V/m)	Ey(V/m)	Ez(V/m)	Em(V/m)
-2.808E-01	2.846E-01	1.930E+00	-1.617E+15	6.209E+14	5.365E+16	5.368E+16

Field values on surface: Locate or enter position >

Figure 18: Values for chosen point on surface

The value of E_m , magnitude of the electric field, from Figure 19 is $5.368E+16$ V/m and it can be seen in the graph below. The graph displays the electric field strength from top to bottom of the front view on the outside of the enclosure.

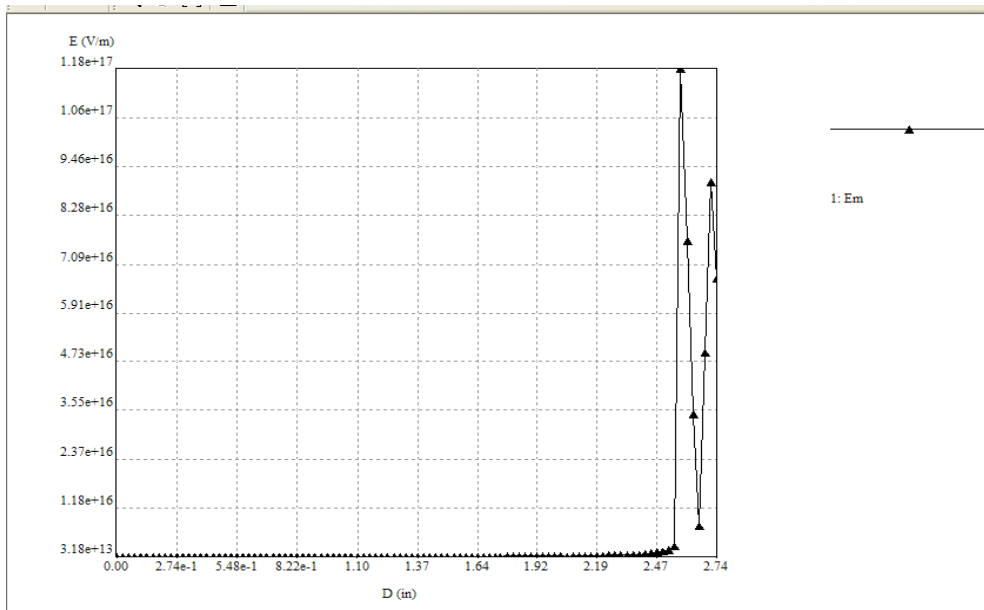


Figure 19: Graph of front

The applied field for the aluminum in the y direction is given below in Figure 21.

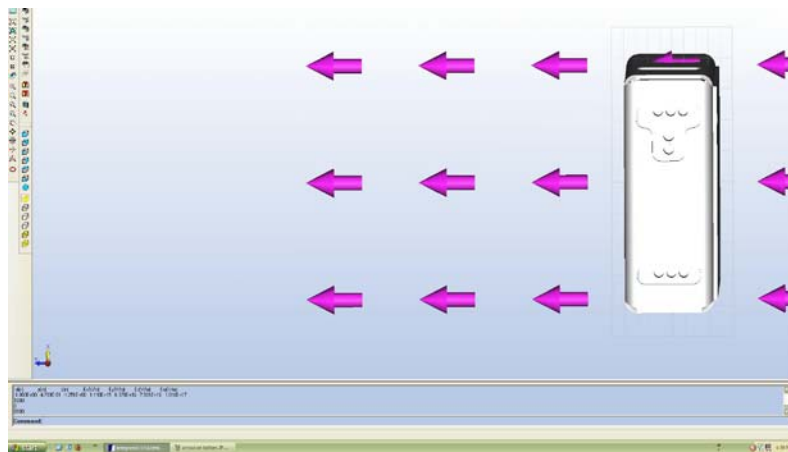


Figure 20: Aluminum Impressed y E-field

In Figure 22, the arrows are shown to express the electric field strengths at the front of the enclosure. The arrow colors range from blue to red, blue being the lowest electric field strength and red being the highest.

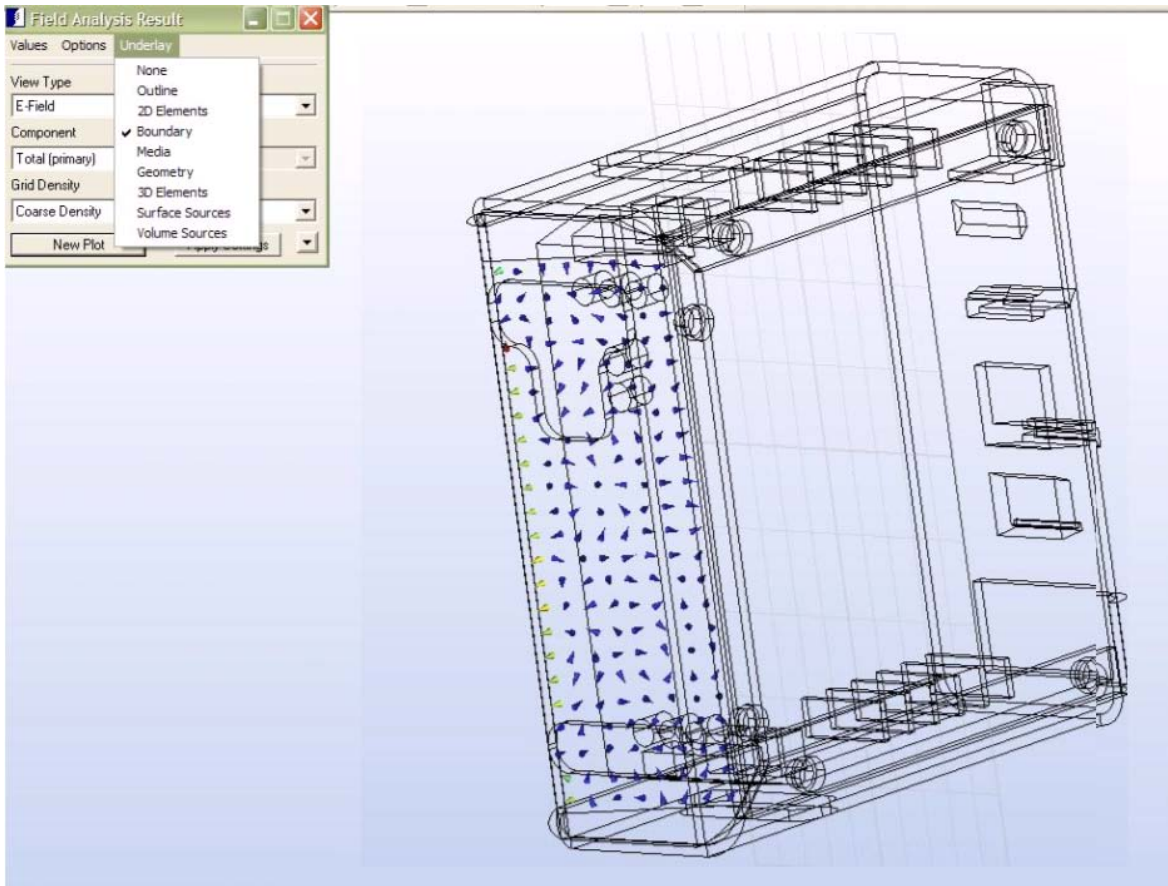


Figure 21: Arrows of electric field strength

In Figure 23 the field analysis result is solving for the electric field at a point on any surface. The values shown at the bottom of the screen display the electric field in the x, y and z directions and the magnitude.

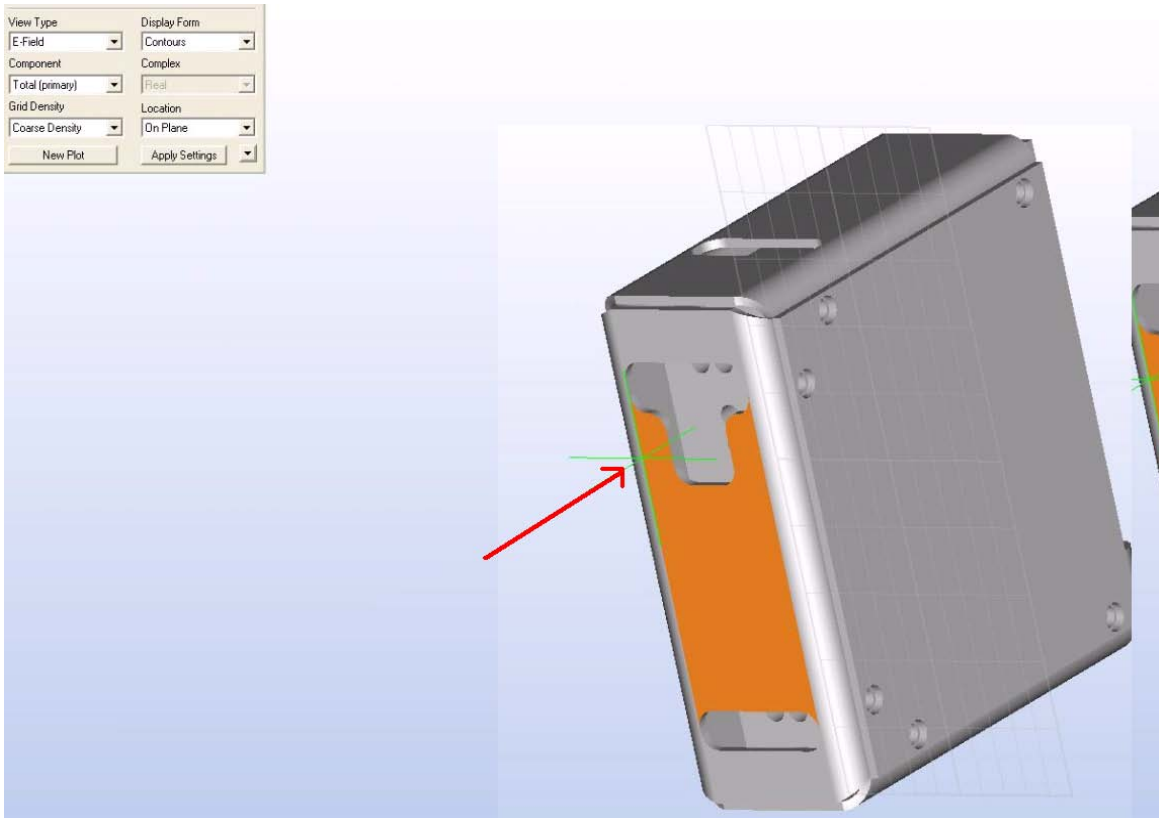


Figure 22: Chosen value on surface

The green point on the surface shows the values of the electric field that are in Figure 24 below.

-2.046E+00	5.361E-01	-1.318E-02	4.560E+13	6.575E+16	-8.813E+12	6.575E+16
x(in)	y(in)	z(in)	Ex(V/m)	Ey(V/m)	Ez(V/m)	Em(V/m)
-1.704E+00	-4.709E-01	-4.763E-01	6.086E+14	-7.749E+14	1.476E+13	9.854E+14
x(in)	y(in)	z(in)	Ex(V/m)	Ey(V/m)	Ez(V/m)	Em(V/m)
-7.633E-01	-4.709E-01	-3.544E-01	-6.684E+14	7.165E+14	1.171E+15	1.527E+15

Figure 23: Values from chosen point on surface

The values of E_x , electric field in the x-direction, from Figure 24 are $6.068E+14V/m$ and $-6.684E+14V/m$, it can be seen in the graph below. The graph displays the electric field strength from top to bottom of the front view of the enclosure.

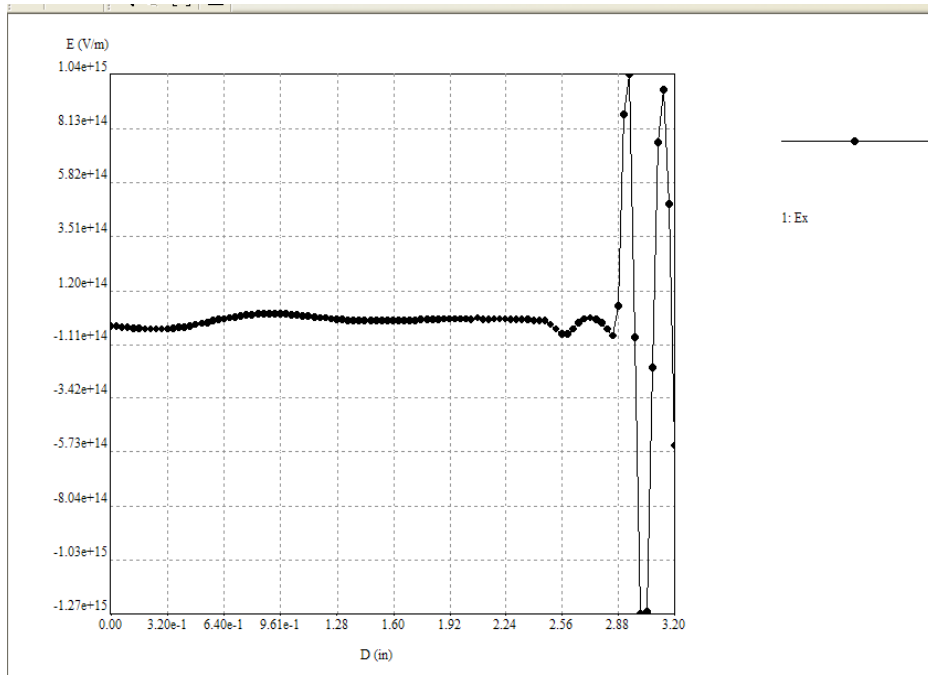


Figure 24: Graph of Front

The applied field for the aluminum in the z direction is given below in Figure 26.

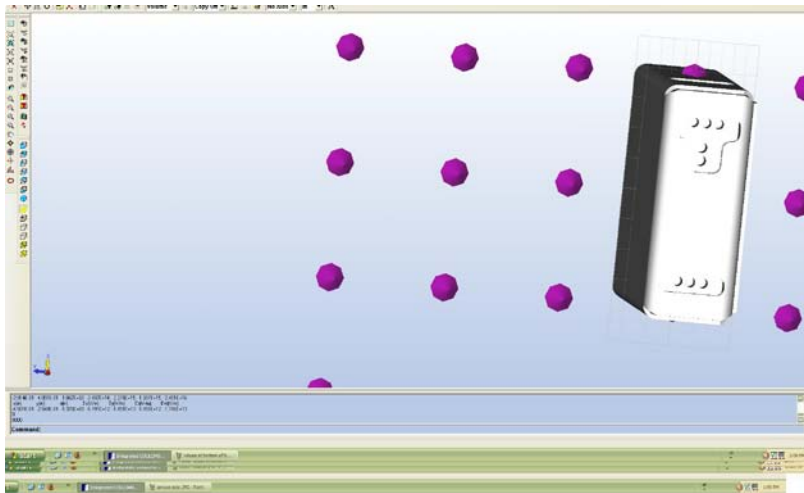


Figure 25: Aluminum Impressed z E-field

In Figure 27 the arrows are shown to express the electric field strengths at the front of the enclosure. The arrow colors range from blue to red, blue being the lowest electric field strength and red being the highest.

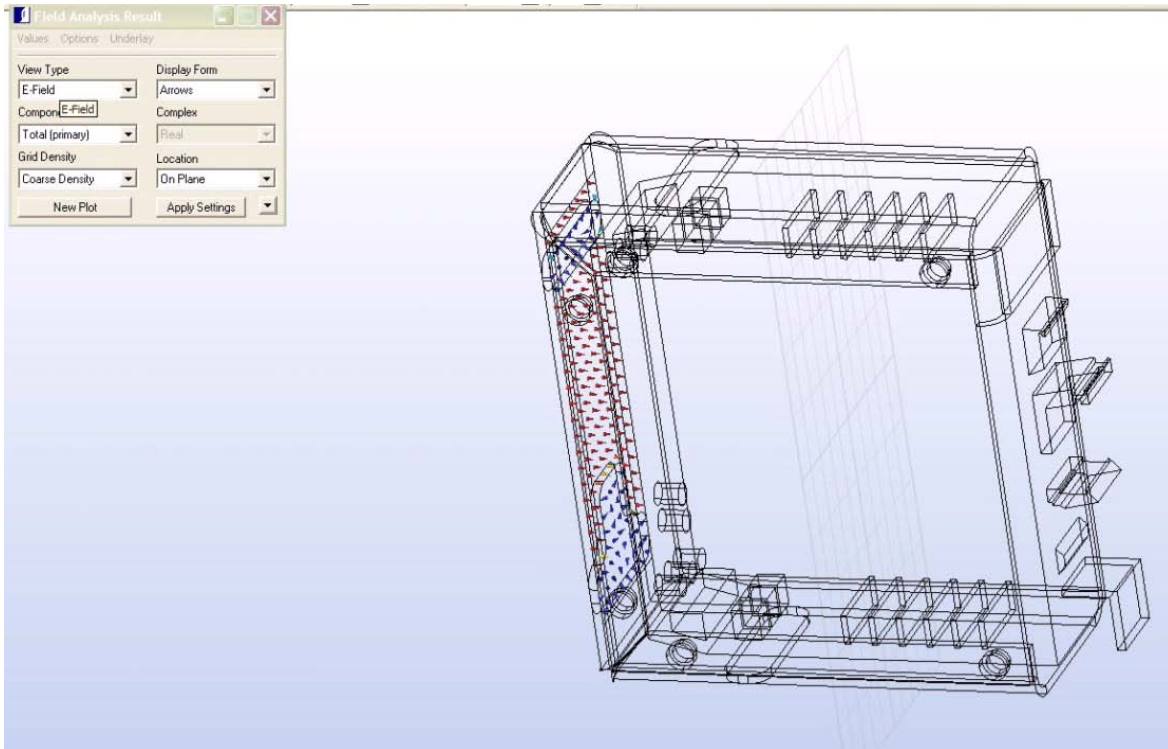


Figure 26: Arrows of electric field strength

In Figure 28 the field analysis result is solving for the electric field at a point on any surface. The values shown at the bottom of the screen display the electric field in the x, y and z directions and the magnitude.

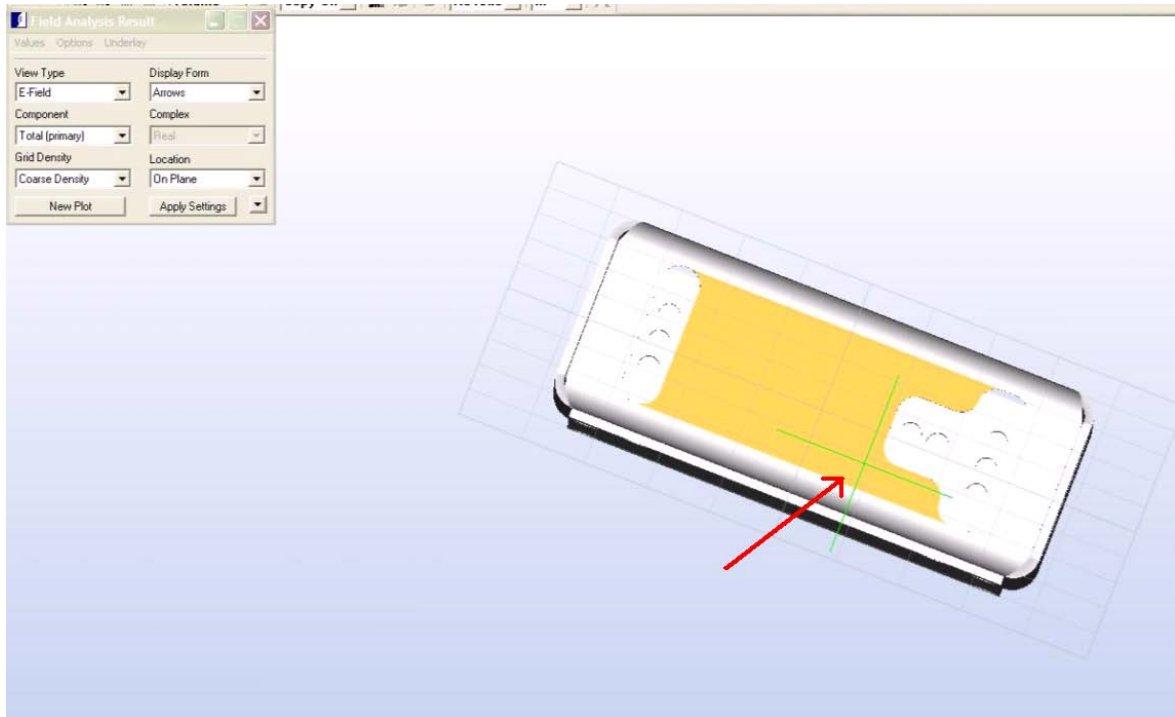


Figure 27: Chosen value on surface

The green point on the surface shows the values of the electric field that are in Figure 29 below.

-3.411E-01	-4.500E-02	1.930E+00	-1.398E+14	-4.590E+14	5.370E+16	5.370E+16
x(in)	y(in)	z(in)	Ex(V/m)	Ey(V/m)	Ez(V/m)	Em(V/m)
-1.837E+00	-2.039E-01	1.930E+00	-3.431E+15	6.893E+15	-3.111E+16	3.205E+16
x(in)	y(in)	z(in)	Ex(V/m)	Ey(V/m)	Ez(V/m)	Em(V/m)
4.236E-01	-2.199E-01	1.930E+00	6.225E+14	-1.504E+16	-1.198E+16	1.924E+16
x(in)	y(in)	z(in)	Ex(V/m)	Ey(V/m)	Ez(V/m)	Em(V/m)
-5.561E-01	7.801E-01	1.930E+00	-6.349E+14	-3.177E+15	5.346E+16	5.356E+16
Coarse density arrows on plane: 192 points on plot. Total number of plots = 1						
Command:						

Figure 28: Values from chosen point on surface

The value of E_x from Figure 29 is $-6.349E+14V/m$, it can be seen in the graph below. The graph displays the electric field strength from top to bottom of the front view of the enclosure.

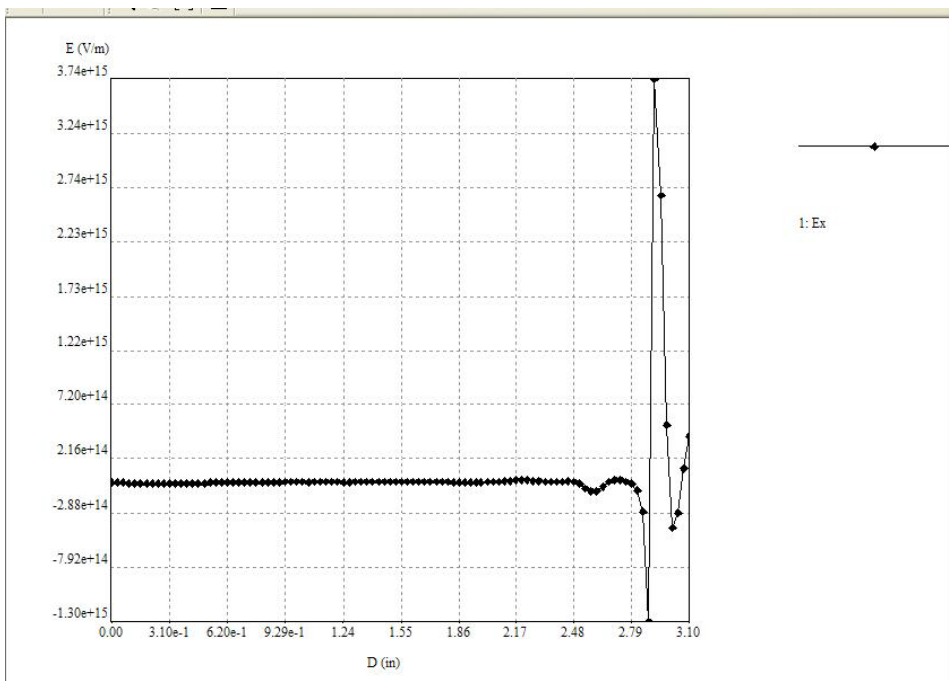


Figure 29: Graph of front

The applied field of the stainless enclosure in the x direction is shown in Figure 31.

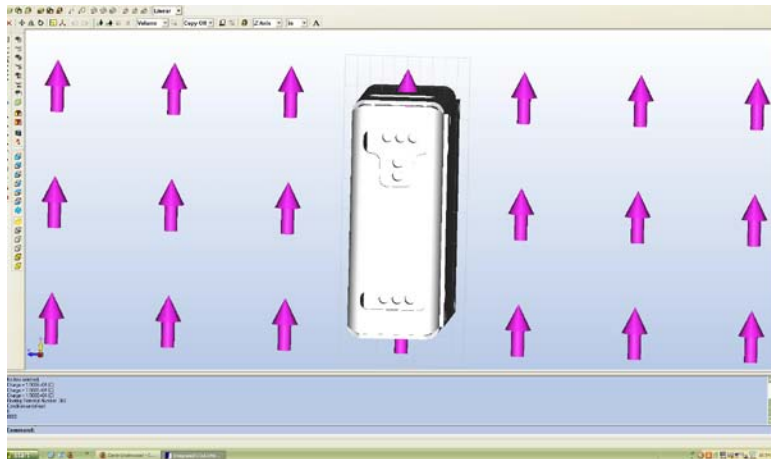


Figure 30: Stainless Impressed x E-field

In Figure 32 the arrows are shown to express the electric field strengths at the front of the enclosure. The arrow colors range from blue to red, blue being the lowest electric field strength and red being the highest.

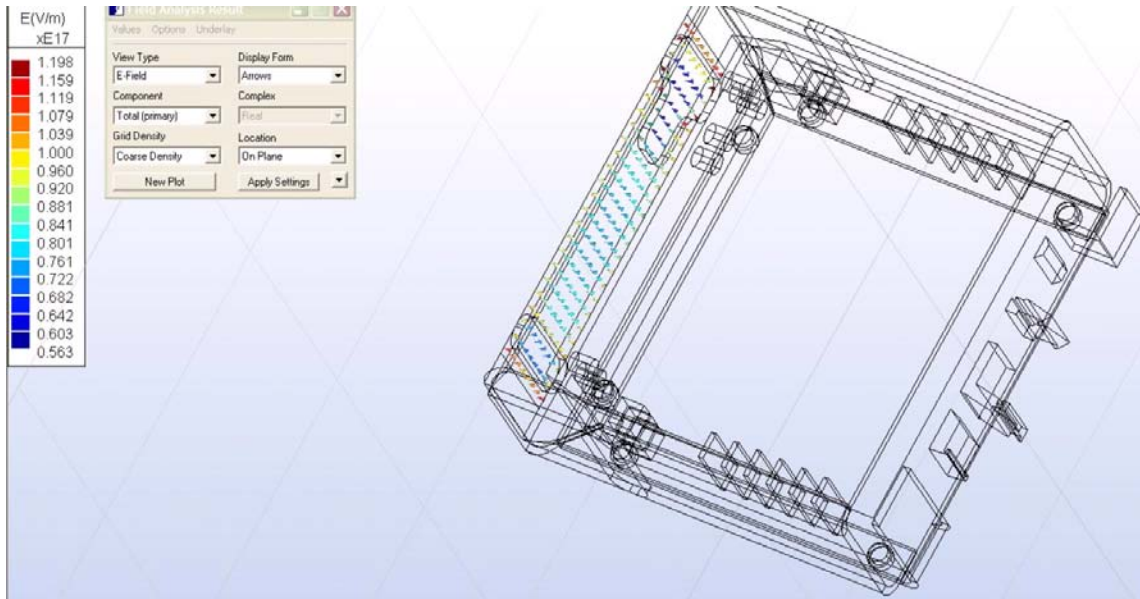


Figure 31: Arrows of electric field strength

In Figure 33 the field analysis result is solving for the electric field at a point on any surface. The values shown at the bottom of the screen display the electric field in the x, y and z directions and the magnitude.

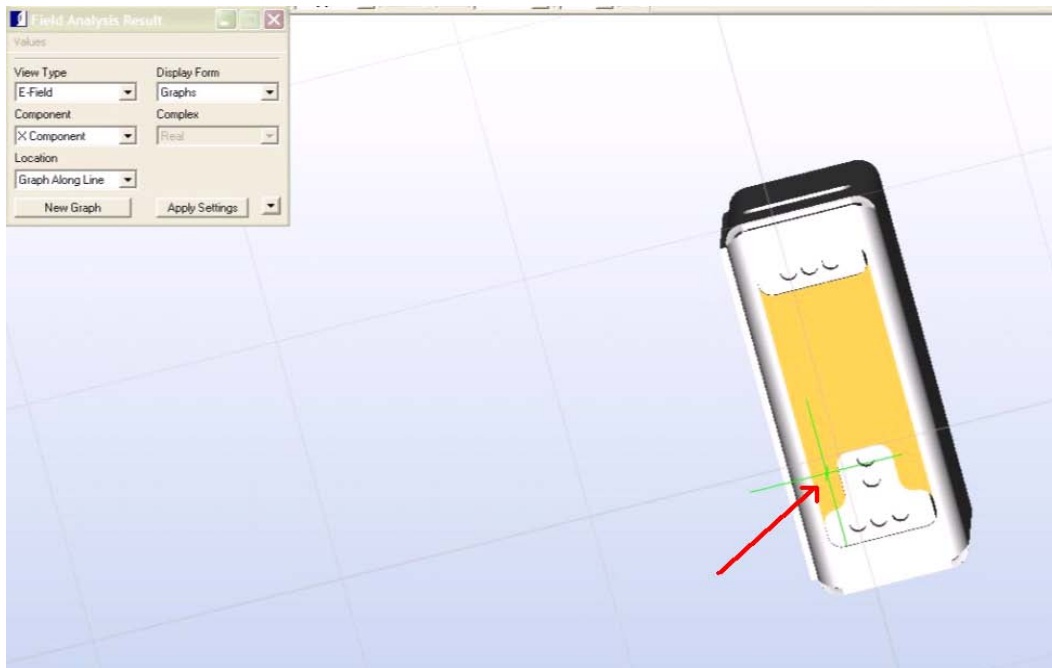


Figure 32: Chosen value on surface

The green point on the surface shows the values of the electric field that are in Figure 34 below.

x(in)	y(in)	z(in)	Ex(V/m)	Ey(V/m)	Ez(V/m)	Em(V/m)
-1.625E+00	-1.083E-01	1.930E+00	-5.812E+14	6.656E+14	5.582E+16	5.583E+16
x(in)	y(in)	z(in)	Ex(V/m)	Ey(V/m)	Ez(V/m)	Em(V/m)
-1.239E+00	4.861E-01	-1.491E+00	1.225E+16	-8.018E+14	-9.086E+16	9.169E+16
x(in)	y(in)	z(in)	Ex(V/m)	Ey(V/m)	Ez(V/m)	Em(V/m)
3.065E-01	4.861E-01	-1.376E+00	5.318E+14	-9.140E+15	-1.723E+17	1.726E+17
x(in)	y(in)	z(in)	Ex(V/m)	Ey(V/m)	Ez(V/m)	Em(V/m)
-5.387E-02	-7.506E-02	1.930E+00	-1.415E+15	-3.247E+15	4.591E+16	4.605E+16

Field values on surface: Locate or enter position >

Figure 33: Values from chosen point on surface

The value of Ex from Figure 34 is 5.318E+14V/m and -1.4515E+15, it can be seen in the graph below. The graph displays the electric field strength from top to bottom of the front view of the enclosure.

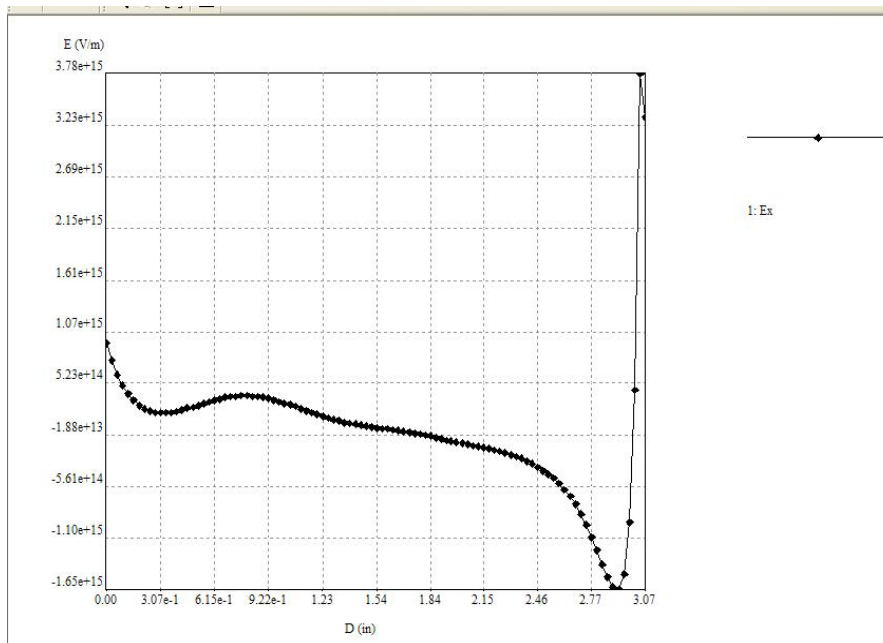


Figure 34: Graph of front

The applied field of the stainless enclosure in the y direction is shown in Figure 36.

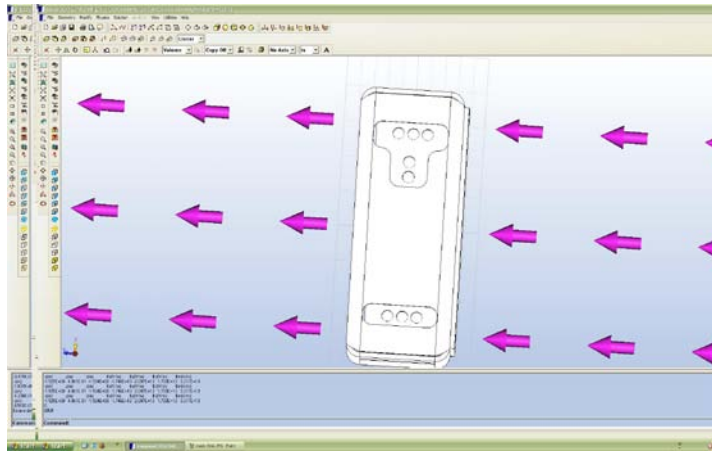


Figure 35: Stainless Applied y E-field

In Figure 37 the arrows are shown to express the electric field strengths at the front of the enclosure. The arrow colors range from blue to red, blue being the lowest electric field strength and red being the highest

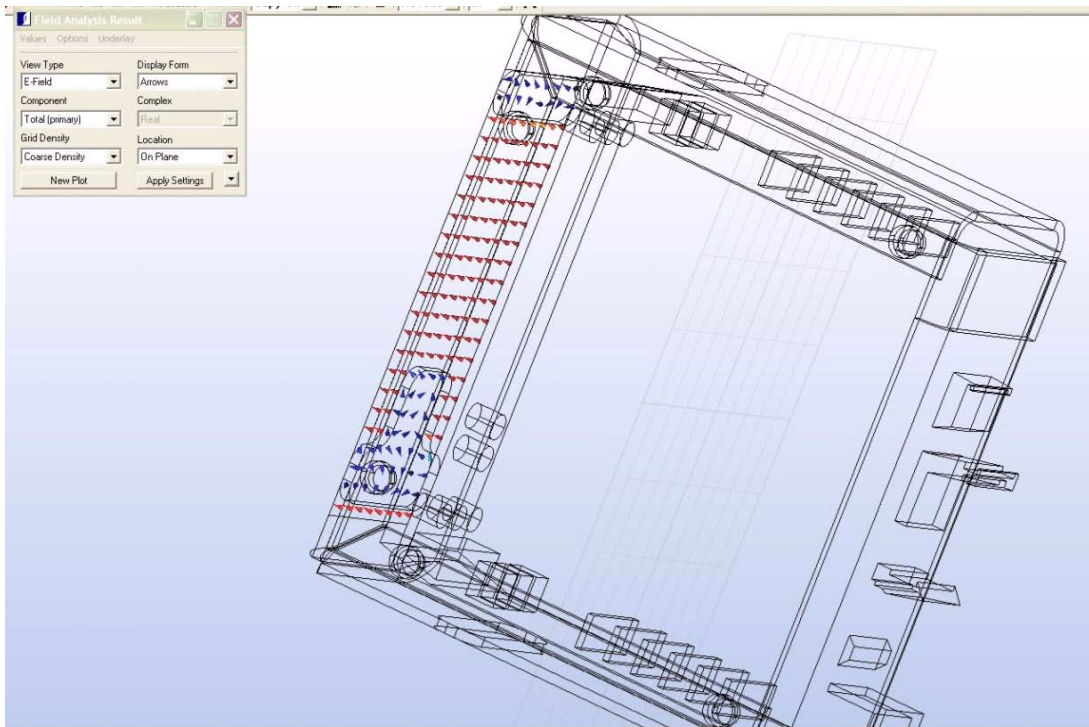


Figure 36: Arrows of electric field strength

In Figure 38 the field analysis result is solving for the electric field at a point on any surface. The values shown at the bottom of the screen display the electric field in the x, y and z directions and the magnitude.

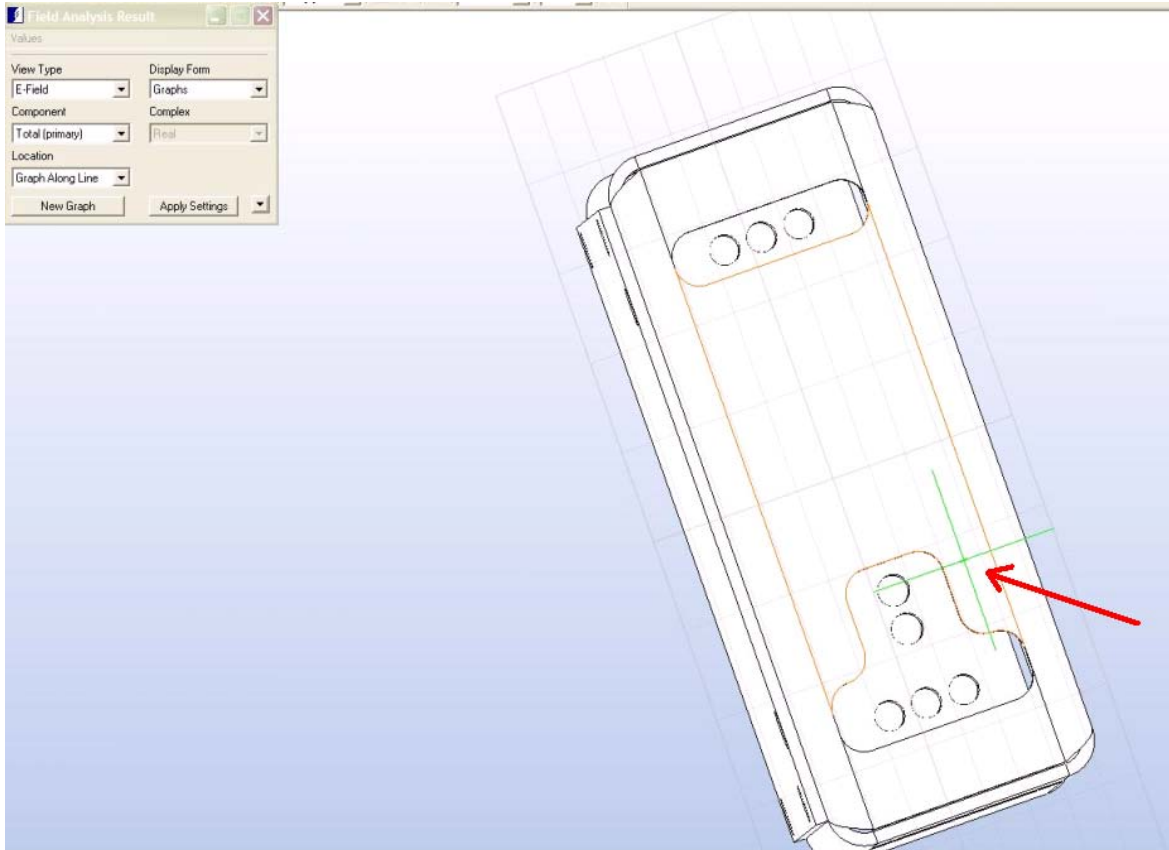


Figure 37: Chosen value on surface

The green point on the surface shows the values of the electric field that are in Figure 39 below.

x(in)	y(in)	z(in)	Ex(V/m)	Ey(V/m)	Ez(V/m)	Em(V/m)
-1.474E+00	-3.279E-02	1.930E+00	1.577E+13	-2.049E+14	5.314E+16	5.314E+16
x(in)	y(in)	z(in)	Ex(V/m)	Ey(V/m)	Ez(V/m)	Em(V/m)
-1.506E+00	6.333E-01	1.930E+00	9.383E+13	5.633E+13	5.390E+16	5.390E+16
x(in)	y(in)	z(in)	Ex(V/m)	Ey(V/m)	Ez(V/m)	Em(V/m)
-1.778E-01	-6.803E-02	1.930E+00	-4.184E+14	-1.370E+15	5.411E+16	5.412E+16
x(in)	y(in)	z(in)	Ex(V/m)	Ey(V/m)	Ez(V/m)	Em(V/m)
-7.915E-02	6.409E-01	1.930E+00	5.107E+13	6.631E+14	5.384E+16	5.384E+16

Field values on surface: Locate or enter position >

Figure 38: Values from chosen point on surface

The value of E_x from Figure 39 is $5.107E+13V/m$, it can be seen in the graph below. The graph displays the electric field strength from top to bottom of the front view of the enclosure.

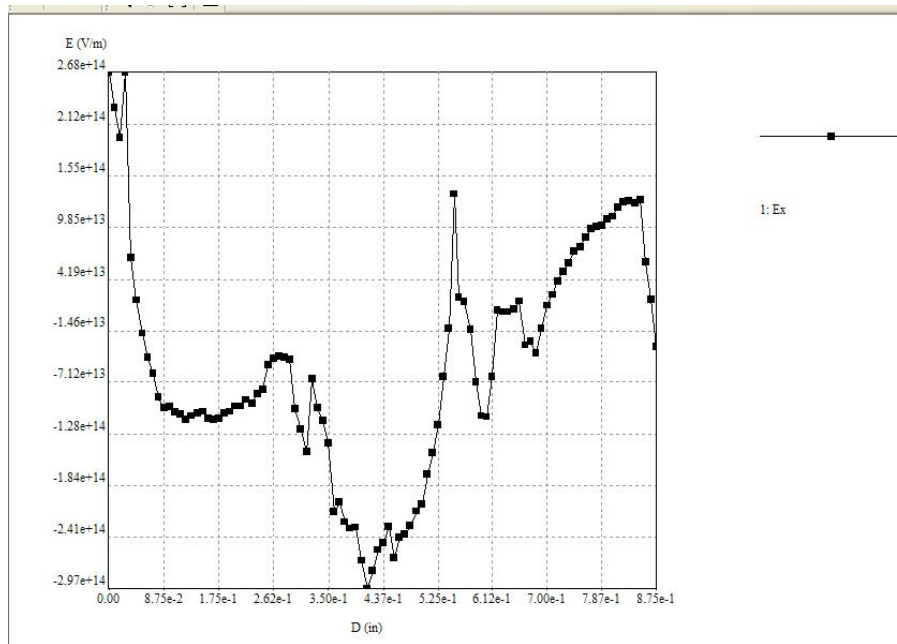


Figure 39: Graph of front

In Figure 41 the arrows are shown to express the electric field strengths at the front of the enclosure in the z direction. The arrow colors range from blue to red, blue being the lowest electric field strength and red being the highest.

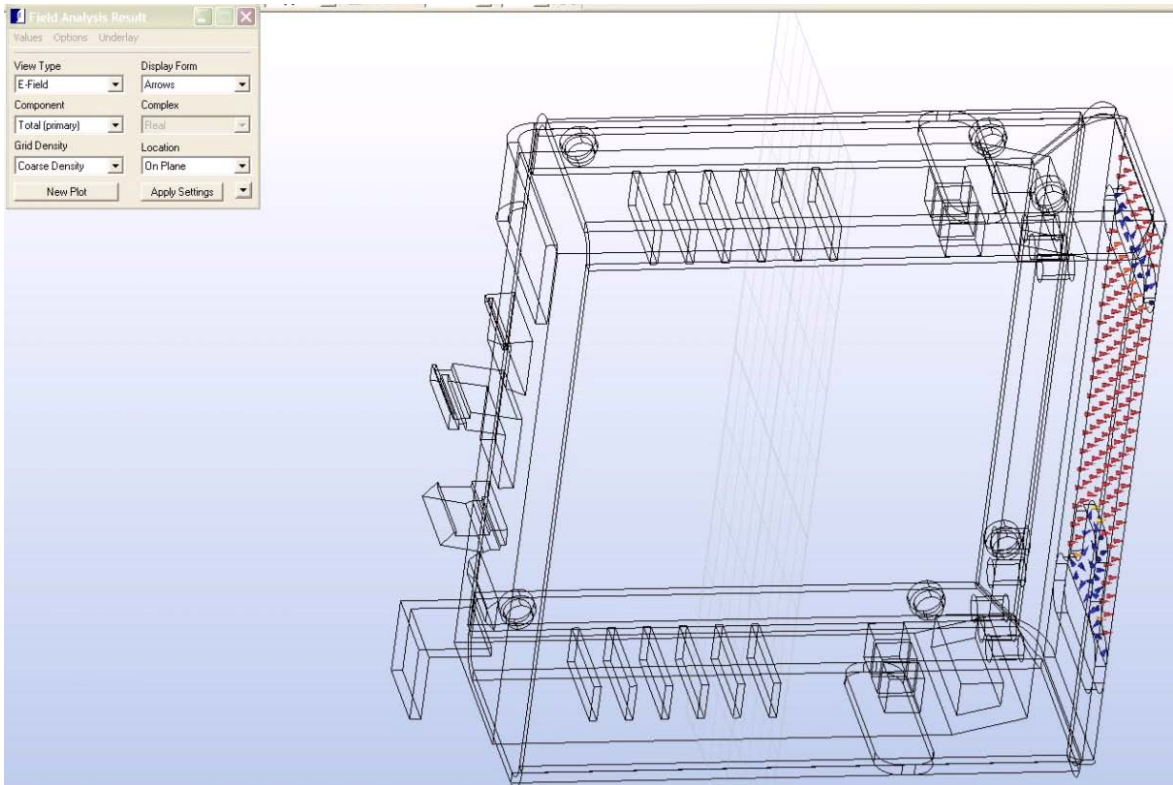


Figure 40: Arrows of electric field strength

In Figure 42 the field analysis result is solving for the electric field at a point on any surface. The values shown at the bottom of the screen display the electric field in the x, y and z directions and the magnitude.

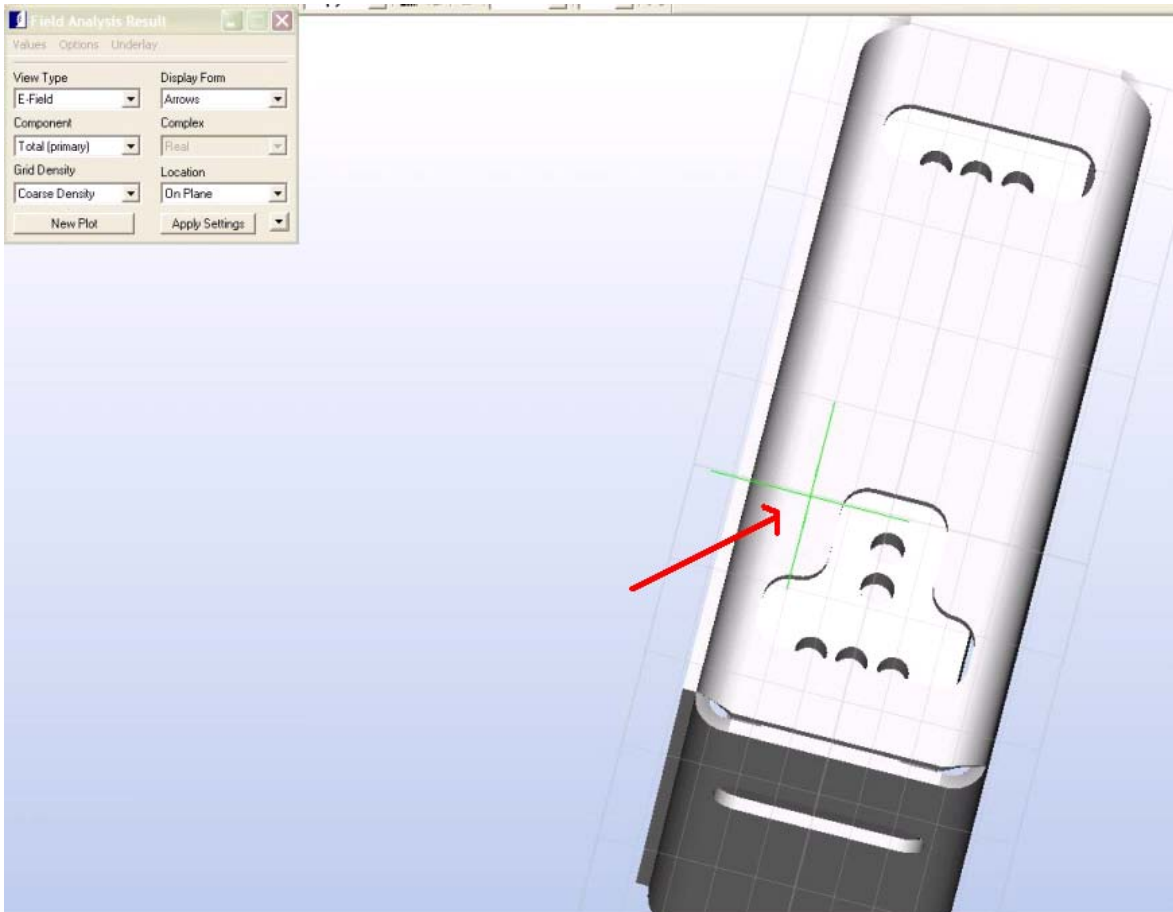


Figure 41: Chosen value on surface

The green point on the surface shows the values of the electric field that are in Figure 43 below.

x(in)	y(in)	z(in)	Ex(V/m)	Ey(V/m)	Ez(V/m)	Em(V/m)
-2.261E+00	-3.890E-02	-2.102E-01	-1.754E+13	-5.341E+12	-1.229E+16	1.229E+16
x(in)	y(in)	z(in)	Ex(V/m)	Ey(V/m)	Ez(V/m)	Em(V/m)
-1.549E+00	6.272E-01	1.930E+00	6.491E+13	4.697E+13	5.401E+16	5.401E+16
x(in)	y(in)	z(in)	Ex(V/m)	Ey(V/m)	Ez(V/m)	Em(V/m)
-2.497E-01	6.748E-01	1.930E+00	6.921E+13	-3.754E+14	5.413E+16	5.414E+16
x(in)	y(in)	z(in)	Ex(V/m)	Ey(V/m)	Ez(V/m)	Em(V/m)
-8.931E-02	-1.214E-01	1.930E+00	-4.588E+14	2.448E+14	5.298E+16	5.299E+16

Locate or enter position >

Figure 42: Values from chosen point on surface

The value of E_x from Figure 43 is $6.921E+13V/m$ and $-4.588E+14$, it can be seen in the graph below. The graph displays the electric field strength from top to bottom of the front view of the enclosure.

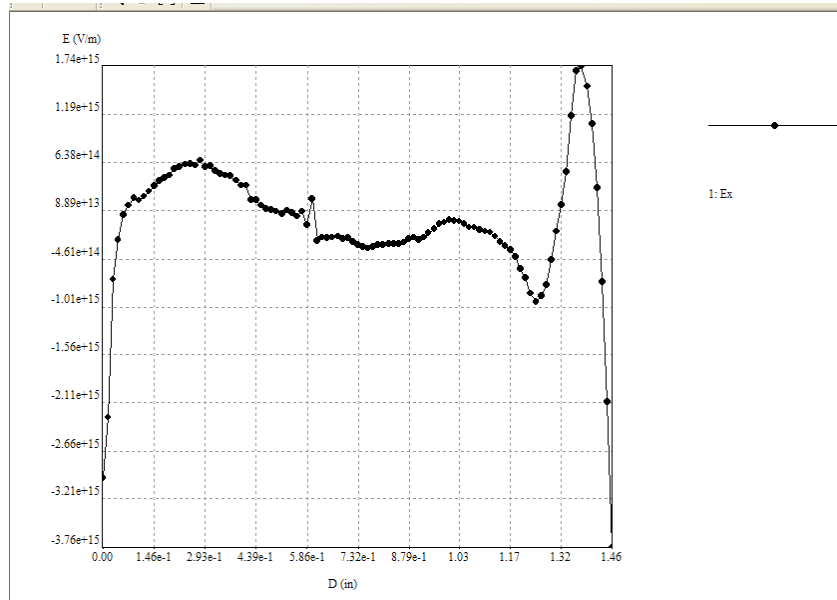


Figure 43: Graph of front

In Table 1 below the values of the aluminum and stainless steel electric field strength is compared. Although the electric field strength does not differ by much between the aluminum and stainless steel, the lower the electric field strength the lower the chance of a module to be affected. Since the enclosures are both grounded the electric field will automatically go to ground.

Impressed Field	Aluminum	Stainless Steel
E_x	$-1.617E+15$	$5.318E+14$
E_y	$6.068E+14$	$5.107E+13$
E_z	$-6.349E+14$	$6.921E+13$

Table 1: Electric Field Strength of Aluminum and Stainless Steel

After using COULOMB I learned a lot about the software and what it can perform. The results that were shown above are only a few solutions to what this software can solve. In general modeling is pretending to work with a real scenario while only working an imitation that can be performed by software tools. It is important to run tests to predict what the outcome that can then be compared to the actual results.

6. Results

6.1 Introduction

The following results were provided from Westinghouse Electric Company and the testing was conducted in New Stanton, PA. The standard used for the Electrostatic testing for the modules was the European Standard EN61000-4-2 “Testing and Measurement Techniques Electrostatic Discharge Immunity Test” The scope of this standard relates to the immunity requirements and test methods for electrical and electronic equipment that are subjected to static electricity discharge. The standard also defines ranges of the test levels and establishes test procedures.

The test setup for ESD testing is straightforward. The equipment under test is placed over a ground surface as shown in Figure 46, which is the ground lead. This test setup consists of a non-conductive table standing on the ground reference plane. A horizontal coupling plane is placed on the table. The equipment under test is isolated from the coupling plane by an insulating support. The ground lead is kept away from the equipment under test by at least 200mm. The distance between the ground plane and the equipment under test should be kept 100mm from the floor and 800mm from the table-top.

The procedure of the testing includes both the contact and air discharge by using interchangeable metal tips. For contact discharge, the pointed tip is contacted with the testing point, and a high voltage within the units is applied to discharge to the contact

point. For air discharge, a rounded tip is used with a high-voltage and then released by a spark. Air discharge is mostly tested for plastic enclosures where there are gaps.

Contact discharge		Air discharge	
Level	Test voltage kV	Level	Test voltage kV
1	2	1	2
2	4	2	4
3	6	3	8
4	8	4	15
x ^a	Special	x ^a	Special

^a "x" can be any level, above, below or in between the others. The level shall be specified in the dedicated equipment specification. If higher voltages than those shown are specified, special test equipment may be needed.

Figure 44: Test Levels

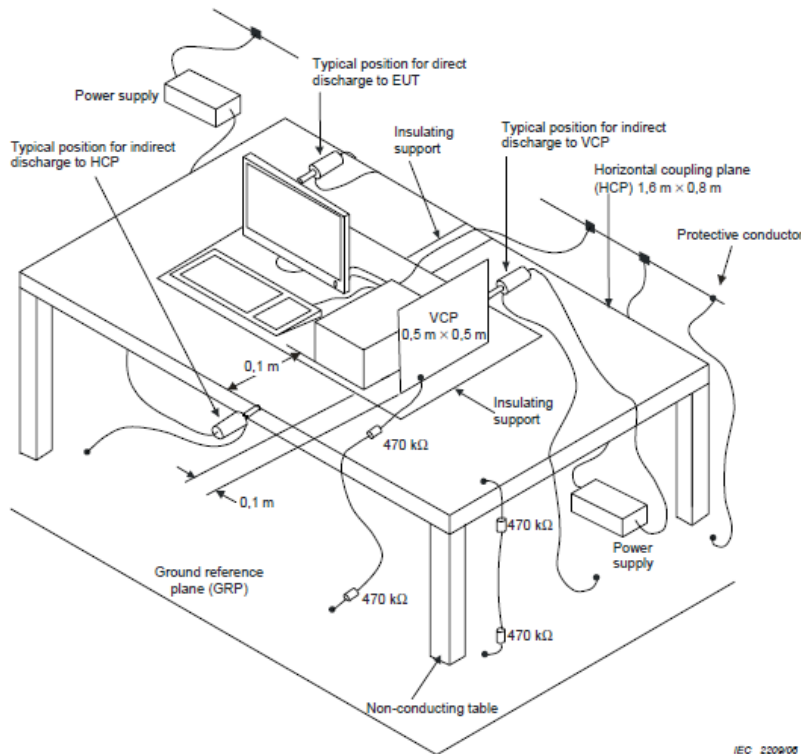


Figure 45: Set-up of test bench

6.2 ESD Test Results

6.2.1 Modules

The modules supplied from Acromag are tested to a certain level without any enclosure. According to the data sheets provided for the modules which were tested up to 4kV direct contact and 8kV air-discharge and passed. Before the modules were tested they were powered up and were tested for functionality. The output values of the modules were monitored with a Fluke 2640A NetDAQ (Networked Data Acquisition Unit) data logger and with the equipment used by the testing engineer.

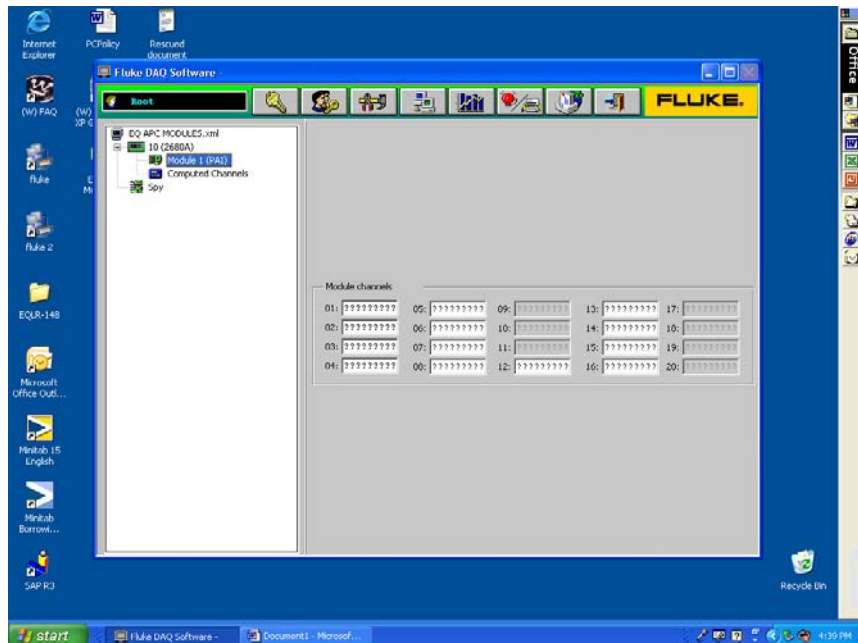


Figure 46: Data Logger Software

The electrostatic discharge immunity testing began with level 1 contact and then level 1 air discharge. The testing continues until one or more modules fail either by losing power or not reading the expected output at the data logger. The modules did pass at level 2 for contact and level 3 for air-discharge as noted in the data sheet. The jump to the next level

where contact was 8kV, where the modules all failed to read the expected output values and a few of the modules lost power and were damaged. Since the modules were plastic they were also tested for air-discharge at level 4 (15kV) and the modules failed.

Unfortunately the output results without the enclosures were not provided since they failed immediately.

6.2.2 Aluminum Enclosure

The aluminum enclosure was tested with module W5207 since it's the most common module that is used. Since the enclosures were metal, the charge was applied by direct contact with the metal at 8kV. The module was tested at level 1, 2 and 4 for contact discharge. The acceptance range for this module was 117.440 – 122.560 mV.

W5207 Aluminum Enclosure		
Level	Output	Pass/Fail
2kV	120.69mV	Pass
4kV	120.80mV	Pass
8kV	120.74mV	Pass

Table 2: Results for Aluminum

The table above shows that the enclosure designed for these modules passed testing for the highest level of discharge.

6.2.3 Stainless Steel Enclosure

The same procedure was repeated for the stainless steel enclosure. The acceptance criteria range was the same, 117.440-122.560mV.

W5207 Stainless Enclosure		
Level	Output	Pass/Fail
2kV	120.41mV	Pass
4kV	120.49mV	Pass
8kV	120.04mV	Pass

Table 3: Results for Stainless Steel

The table above shows that the enclosure design for the stainless steel also passed for the highest level of discharge.

6.3 Compare Software and Testing Results

To evaluate the software results the electric field strength of the aluminum and stainless steel is compared. When compared, the lower the electric field strength registers at the enclosure, there becomes a lower chance of the module being affected. As seen in Table 1, stainless steel registers lower electric field strength across the front of the enclosure.

The testing results shown in Table 2 and Table 3 are the outputs in millivolts that are recorded as the contact discharge is applied. The acceptance range is between 117.440 and 122.560mV. To calculate the exact expected output the mean of the values are calculated, which is exactly 120mV. Aluminum is 0.7mV to 0.8mV higher than the exact expected output where stainless steel is .04mV to .5mV higher than the exact expected output. This concludes that the stainless steel was more successful than the aluminum enclosure.

7. Conclusions

I conclude this MQP Report by summarizing the steps that were taken to complete this project. The design of the final wiring diagram and the set up of all modules was mounted into the cabinet. The aluminum and stainless steel enclosures were important to protect the modules from high electrostatic discharge. The modules were only tested at medium level and needed to pass the highest level. Numerical software was conducted to predict the field distribution for the enclosure in orthogonal directions. The software was important to predict if the modules would pass. The modules were then manufactured after being designed in SolidWorks at the machine shop at Worcester Polytechnic Institute in both aluminum and stainless steel. After the enclosures were completed they were sent down to testing that was conducted in New Stanton, PA by Washington Labs Facility. The data collected for the testing of the modules was then compared to the experimental results of COULOMB.

In this project, it was successfully demonstrated that a metal enclosure can protect an electronic device from electrostatic discharge. With the software and testing analysis that was completed it was demonstrated that the stainless steel enclosure was more successful. It was very important for these modules to maintain functionality at all times since they are a crucial part to a safety system of a Nuclear Power Plant.

I suggest for any future work that may include the design of an enclosure for an electric component that it is more carefully designed to perfectly enclose the component. Due to limited supplies in the machine shop it was impossible to get a perfect box enclosure to not

have any openings or imperfections. I recommend that the enclosure is professionally made to have a better final product that may be used in the market.

References

1. Hayt, William. *Engineering Electromagnetics*, Purdue University: 1974. 3rd Edition.
2. Marshall, Stanley, and Gabriel Skitek. *Electromagnetic Concepts and Application*. New Jersey: 1990, 3rd Edition.
3. Baxleitner, Warren. *Electrostatic Discharge and Electronic Equipment: A Practical Guide for Designing to Prevent ESD Problems*, Wiley-IEEE Press. 1999.
4. European Standard IEC 61000-4-2:2008, “Electromagnetic Compatibility- Part 4-2: Testing and measurement techniques- Electrostatic Discharge immunity test” 2008.
5. Fundamentals of Electrostatic Discharge, Electrostatic Discharge Association (Electrostatic Discharge Association, 2001)<http://www.esda.org/basics/part1.cfm>
6. M.A. Kelly, G.E Servais and T.V. Pfaffenbach. “An Investigation of Human Body Electrostatic Discharge”, (Delco Electronics, 1993)
< <http://www.aecouncil.com/Papers/aec1.pdf> >

Appendix A: Standards

The following are the codes and standards that direct equipment qualification of the safety-related signal conditioning equipment.

1. IEEE Std 323-1983, "IEEE Standard for Qualifying Class 1E Equipment for Nuclear Power Generating Stations."
2. IEEE Std 344-1987, "IEEE Recommended Practice for Seismic Qualification of Class 1E Equipment for Nuclear Power Generating Stations." (Reference 7)
3. US NRC Regulatory Guide 1.29, Revision 3, "Seismic Design Classification," September 1978. (Reference 13)
4. US NRC Regulatory Guide 1.89, Revision 1, "Environmental Qualification of Certain Electric Equipment Important to Safety for Nuclear Power Plants," June 1984.
5. US NRC Regulatory Guide 1.100, Revision 2, "Seismic Qualification of Electric and Mechanical Equipment for Nuclear Power Plants," June 1988. (Reference 8)
6. US NRC Regulatory Guide 1.180, Revision 1, "Guidelines for Evaluating Electromagnetic and Radio-Frequency Interference in Safety-Related Instrumentation and Control Systems," October 2003.
7. US NRC Regulatory Guide 1.75, Revision 2, "Physical Independence of Electric Systems," September 1978.

Appendix B: Wiring Diagrams For Each Module

Wiring description for the W5206

A 5V source will be used to supply voltage to the input of this module. The positive and negative terminals on the voltage source are connected to their respective positive/negative terminals on the input side of the module. The shielded wire around the input shall be equipment grounded. The 24Vdc, 20A QUINT power supply assembly will be used to power the module. The positive power lead is connected to the positive terminal of the output. The negative power lead is connected to the negative terminal on output load (data logger) and earth ground. The positive terminal on the data logger is connected to the negative terminal on the output side on the W5206.

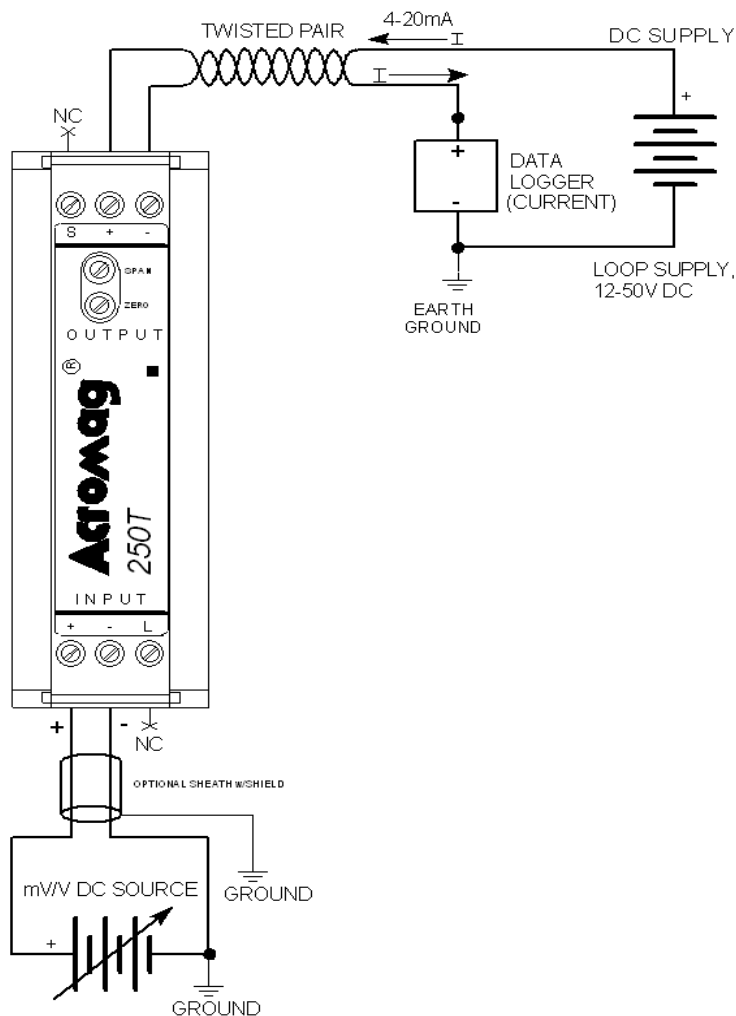


Figure 478 Wiring diagram for the W5206

Wiring description for the W5207

The input signal is set to 50°C using an E type thermocouple simulator. The positive and negative terminals on the thermocouple simulator are connected to their respective positive/negative terminals at the input side of the module using E type thermocouple wire (purple is positive and red is negative). The positive terminal of the module (using a short copper wire) is connected to the “L” terminal of the module. The TC break detection is already installed and in the up position, therefore the input will go high when a break is detected. The negative terminal of the thermocouple simulator is connected to instrument ground. The shielded TC wire around the input shall be equipment grounded. The 24Vdc, 20A QUINT power supply assembly will be used to power the module. The positive power lead is connected to the terminal labeled “P” on the output side. The negative power lead is connected the negative terminal of the output lead (data logger), and the negative terminal of the output side on the module, plus earth ground. The positive terminal of the output load (data logger) is connected to the positive terminal on the output side.

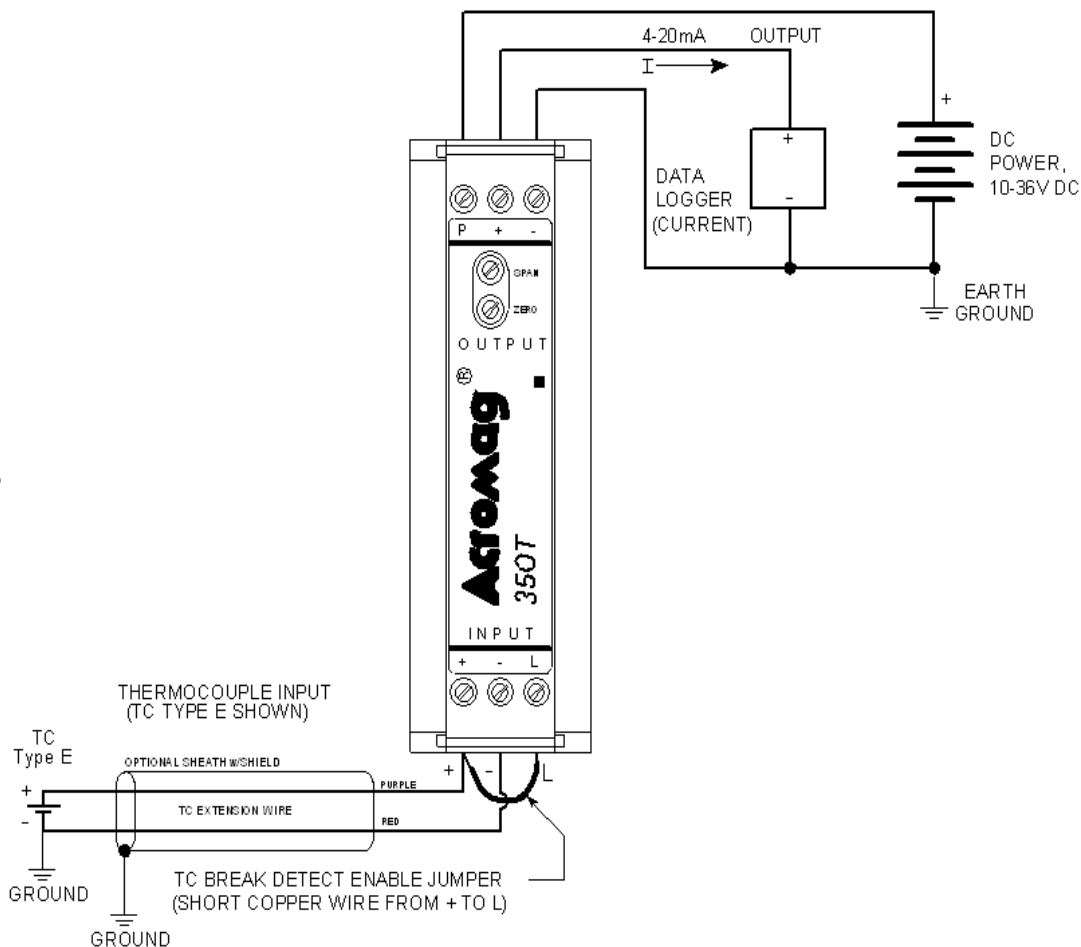


Figure 48 Wiring diagram for the W5207

Wiring description for the W5214

The input signal supplied is set to 100°C using a K type thermocouple simulator. The positive and negative terminals on the thermocouple simulator are connected to their respective positive/negative terminals at the input side of the module using K type thermocouple wire (yellow is positive and red is negative). The positive terminal of the module (using a short copper wire) is connected to the “L” terminal of the module. The TC break detection is already installed and in the up position, therefore the input will go high when a break is detected. The negative terminal of the thermocouple simulator is connected to instrument ground. The shielded TC wire around the input shall be equipment grounded. The 24Vdc, 20A QUINT power supply assembly will be used to power the module. The positive power lead is connected to the terminal labeled “P” on the output side. The negative power lead is connected to the negative terminal of the output load (data logger), and the negative terminal of the output side on the module, plus earth ground. The positive terminal of the output load (data logger) is connected to the positive terminal on the output side.

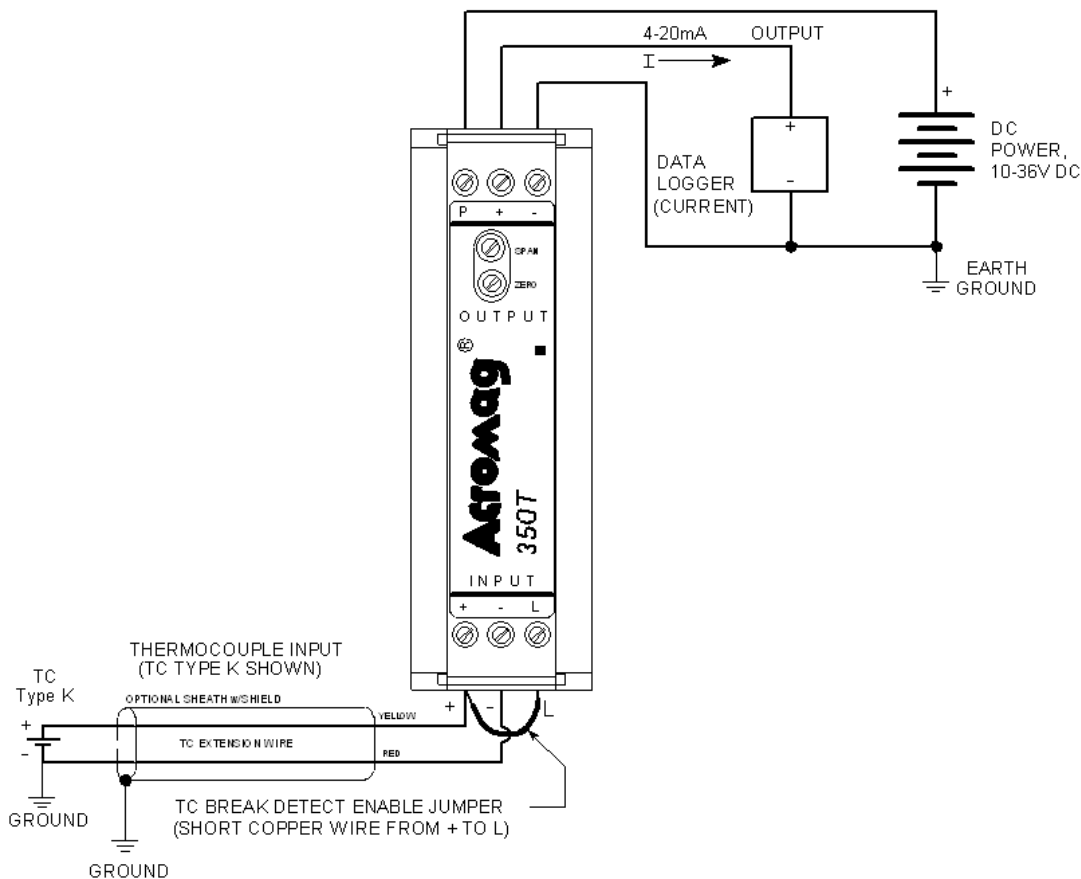


Figure 49 Wiring diagram for the W5207

Wiring description for the W5229

The input signal is set to 30°C using a E type thermocouple simulator. The positive and negative terminals on the thermocouple simulator are connected to their respective positive/negative terminals at the input side of the module using E type thermocouple wire (purple is positive and red is negative). Using copper wire the positive terminal is connected to the “L” terminal. The TC break detection is already installed and in the up position, therefore the input will go high when a break is detected. The negative terminal of the thermocouple simulator is connected to instrument ground. The shielded TC wire around the input shall be equipment grounded. The 24Vdc, 20A QUINT power supply assembly will be used to power the module. The positive power lead is connected to the terminal labeled “P” on the output side. The negative power lead is connected to the negative terminal of the output load (data logger), and the negative terminal of the output side on the module, plus earth ground. The positive terminal of the output load (data logger) is connected to the positive terminal on the output side.

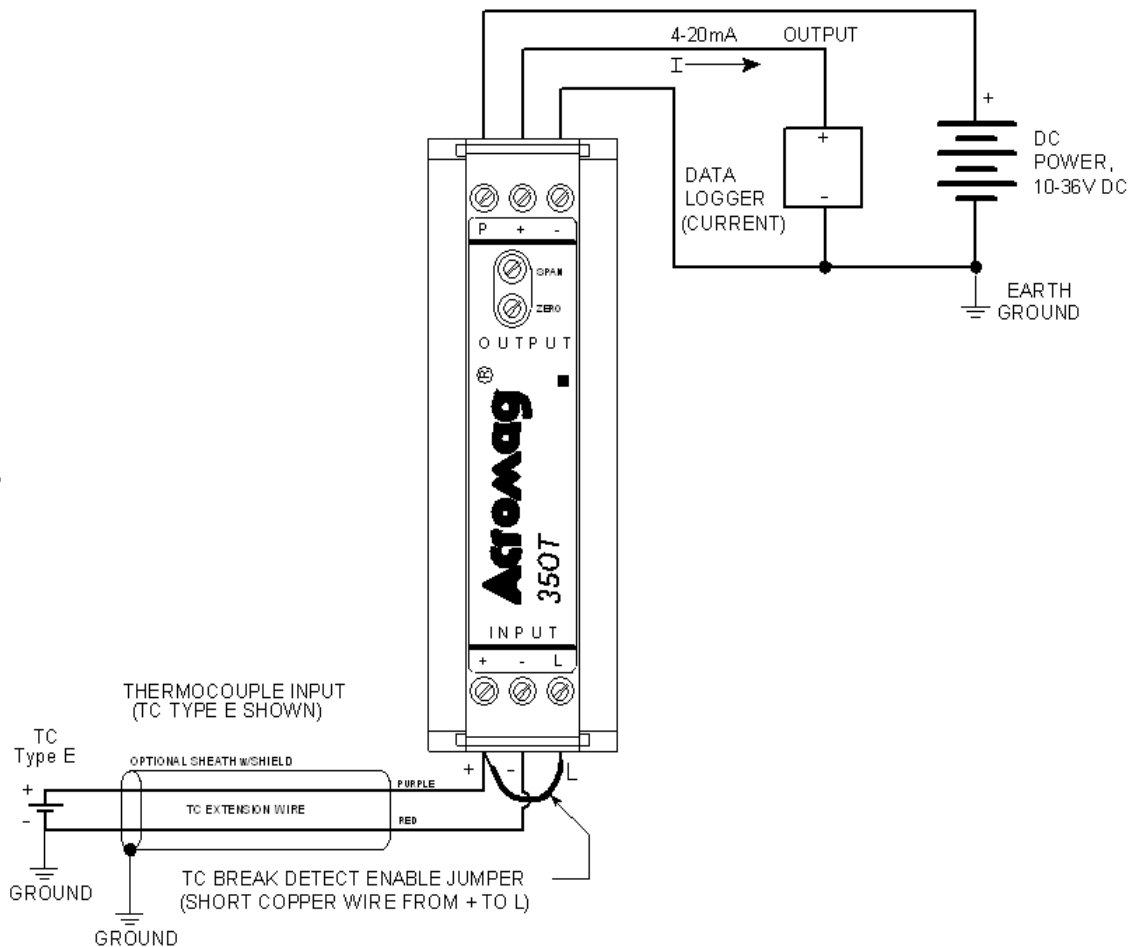


Figure 50 Wiring diagram for the W5229

Wiring description for the W5216

The 2k Ω potentiometer is set to 1k Ω (midpoint). The middle lead on the potentiometer is connected to the “L” terminal. The other two leads on the potentiometer are interchangeable. One lead is connected to the positive terminal and the other is connected to the negative terminal. The negative terminal is connected to instrument ground. The shielded wire around the input shall be equipment grounded. The 24Vdc, 20A QUINT power supply assembly will be used to power the module. The positive power lead is connected to the terminal labeled “P” on the output side. The negative power lead is connected to the negative terminal of the output load (data logger), and the negative terminal of the output side of the module on the module, plus earth ground. The positive terminal of the output load (data logger) is connected to the positive terminal on the output side.

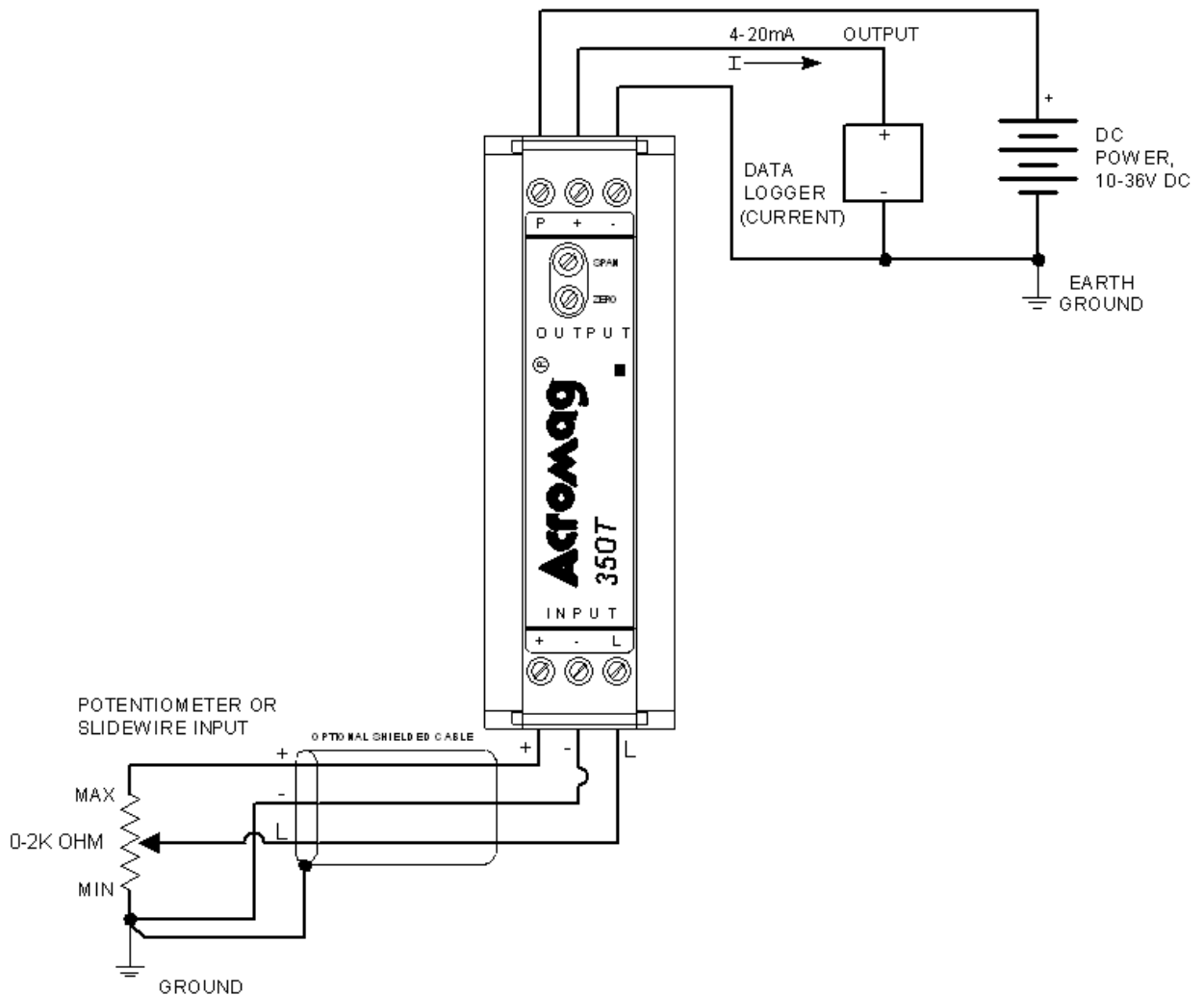


Figure 51 Wiring diagram for the W5216

Wiring description for the W5218

The input signal is given by the RTD simulator using the three (3) input wire configuration. The RTD simulator will be set to 26°C (110.12Ω). The negative terminal is connected to instrument ground. The shielded wire around the input shall be equipment grounded. The 24Vdc, 20A QUINT power supply assembly will be used to power the module. The positive power lead is connected to the terminal labeled “P” on the output side. The negative power lead is connected to the negative terminal of the output load (data logger), and the negative terminal of the output side on the module, plus earth ground. The positive terminal of the output load (data logger) is connected to the positive terminal on the output side.

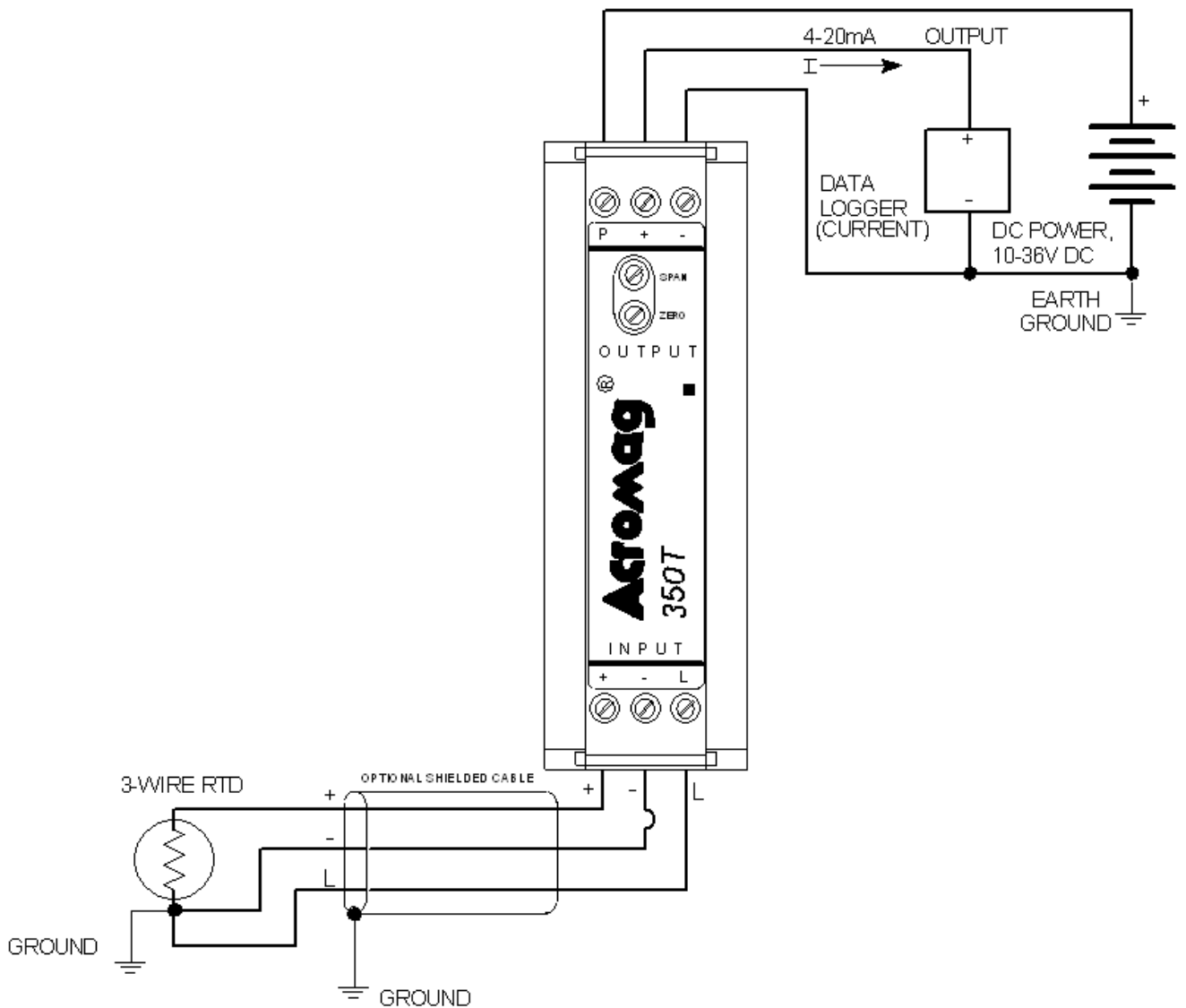


Figure 52 Wiring diagram for the W5218

Wiring description for the W5221

The input signal is given by the RTD simulator using the three (3) input wire configuration. The RTD simulator will be set to 280°C (204.90Ω). The negative terminal is connected to instrument ground. The shielded wire around the input shall be equipment grounded. The 24Vdc 20A QUINT power supply assembly will be used to power the module. The positive power lead is connected to the terminal labeled “P” on the output side. The negative power lead is connected to the negative terminal of the output load (data logger), and the negative terminal of the output side on the module, plus earth ground. The positive terminal of the output load (data logger) is connected to the positive terminal on the output side.

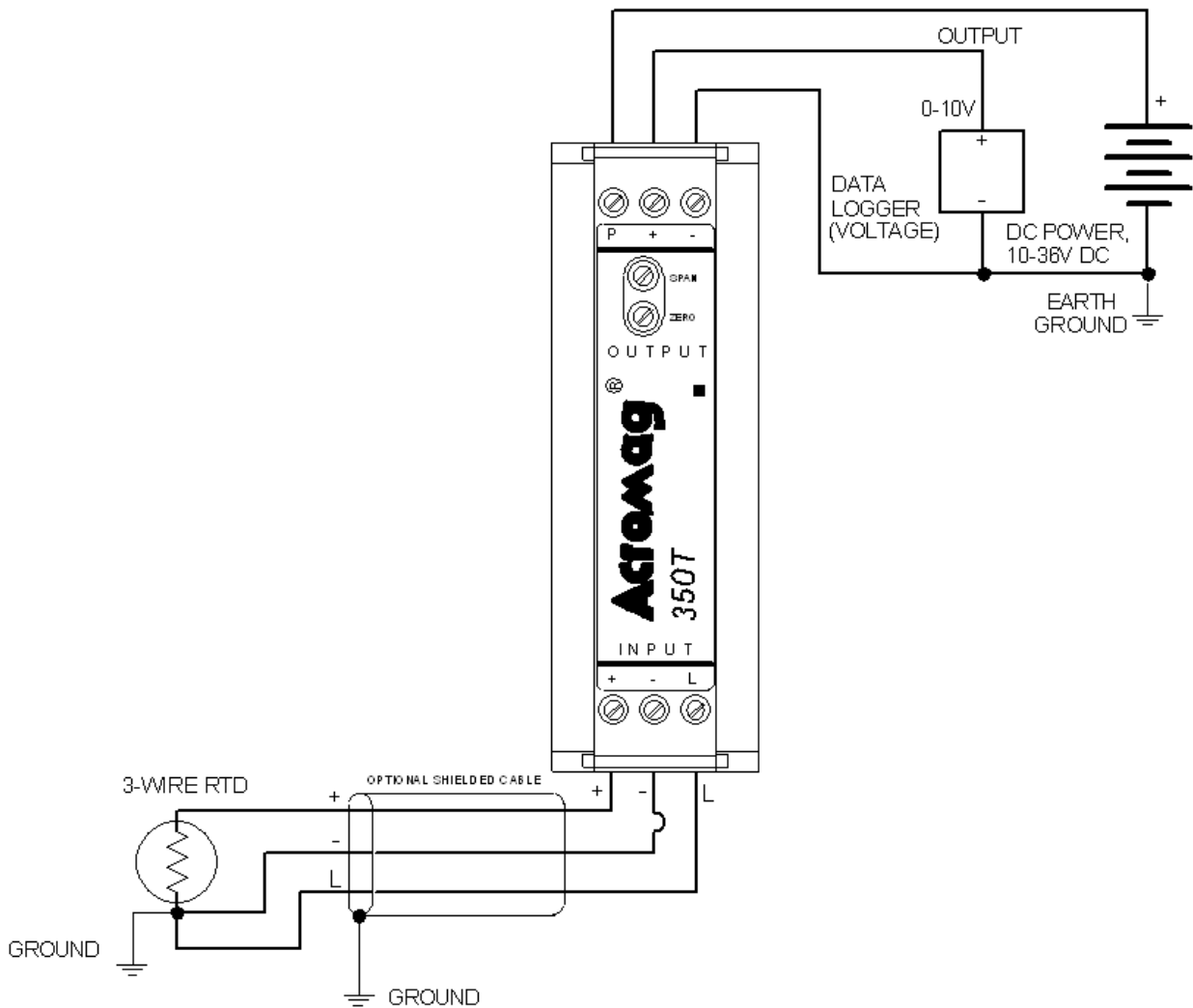


Figure 53 Wiring diagram for the W5221

Wiring description for the W5224

The input signal is given by the RTD simulator using the three (3) input wire configuration. The RTD simulator will be set to 66°C (125.54Ω). The negative terminal is connected to instrument ground. The shielded wire around the input shall be equipment grounded. The 24Vdc 20A QUINT power supply assembly will be used to power the module. The positive power lead is connected to the terminal labeled “P” on the output side. The negative power lead is connected to the negative terminal of the output load (data logger), and the negative terminal of the output side on the module, plus earth ground. The positive terminal of the output load (data logger) is connected to the positive terminal on the output side.

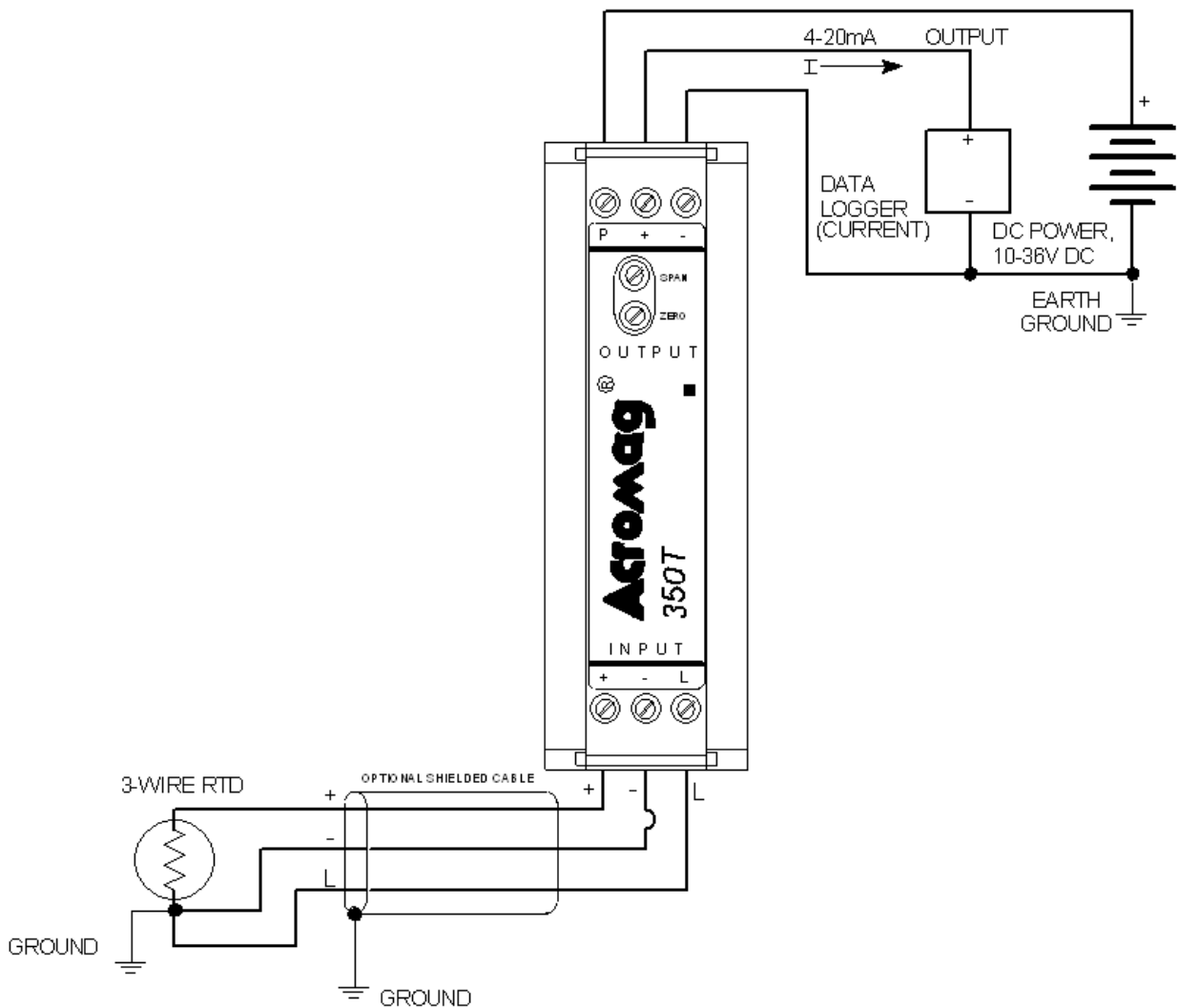


Figure 54 Wiring diagram for the W5224

Wiring description for the W5227

The input signal is given by the RTD simulator using the three (3) input wire configuration. The RTD simulator will be set to 200°C (175.86Ω). The negative terminal is connected to instrument ground. The shielded wire around the input shall be equipment grounded. The 24Vdc, 20A QUINT power supply assembly will be used to power the module. The positive power lead is connected to the terminal labeled “P” on the output side. The negative power lead is connected to the negative terminal of the output load (data logger), and the negative terminal of the output side on the module, plus earth ground. The positive terminal of the output load (data logger) is connected to the positive terminal on the output side.

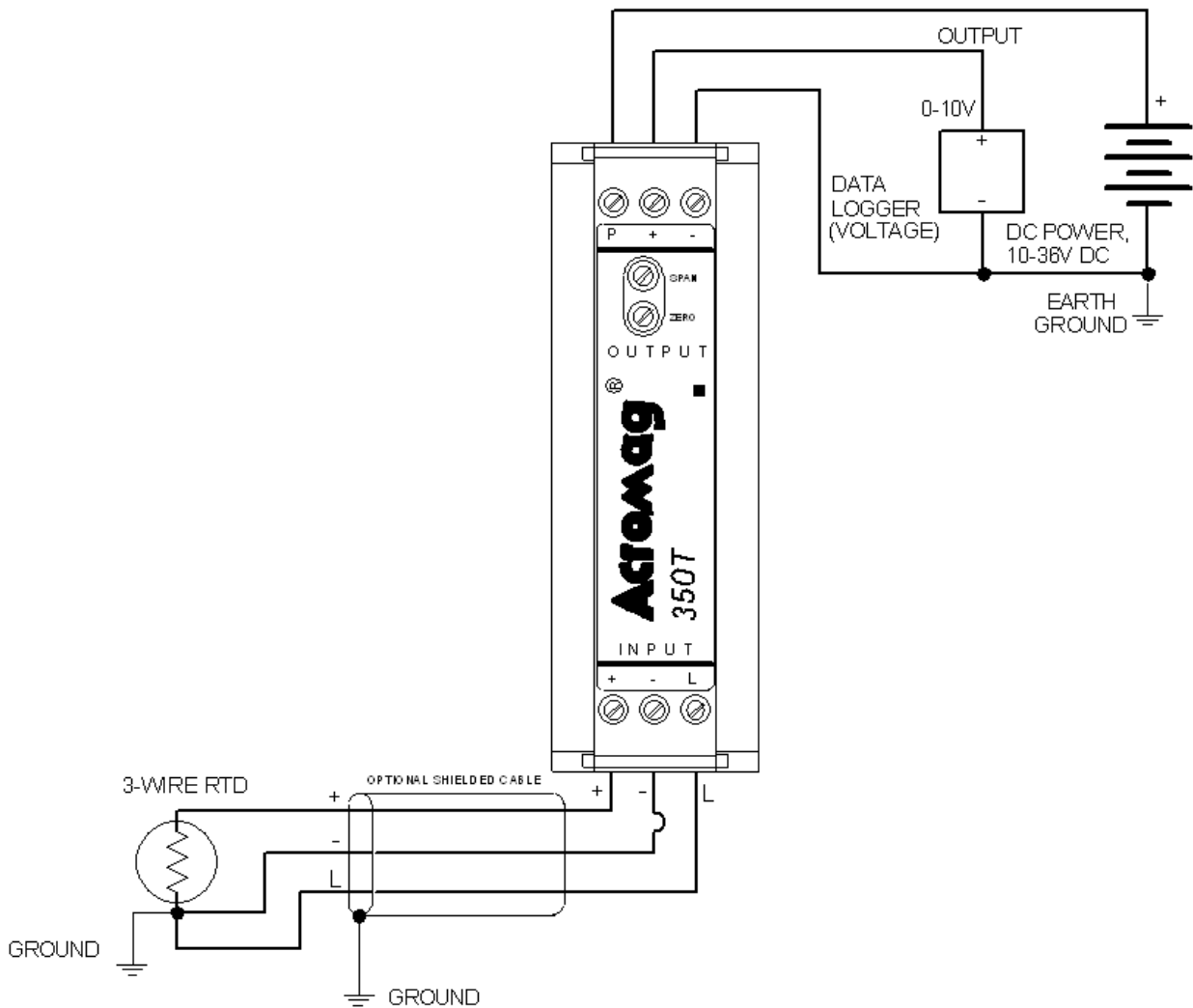


Figure 55 Wiring diagram for the W5227

Wiring description for the W5228

The input signal is given by the RTD simulator using the three (3) input wire configuration. The RTD simulator will be set to 175°C (166.63Ω). The negative terminal is connected to instrument ground. The shielded wire around the input shall be equipment grounded. The 24Vdc 20A QUINT power supply assembly will be used to power the module. The positive power lead is connected to the terminal labeled “P” on the output side. The negative power lead is connected to the negative terminal of the output load (data logger), and the negative terminal of the output side on the module, plus earth ground. The positive terminal of the output load (data logger) is connected to the positive terminal on the output side.

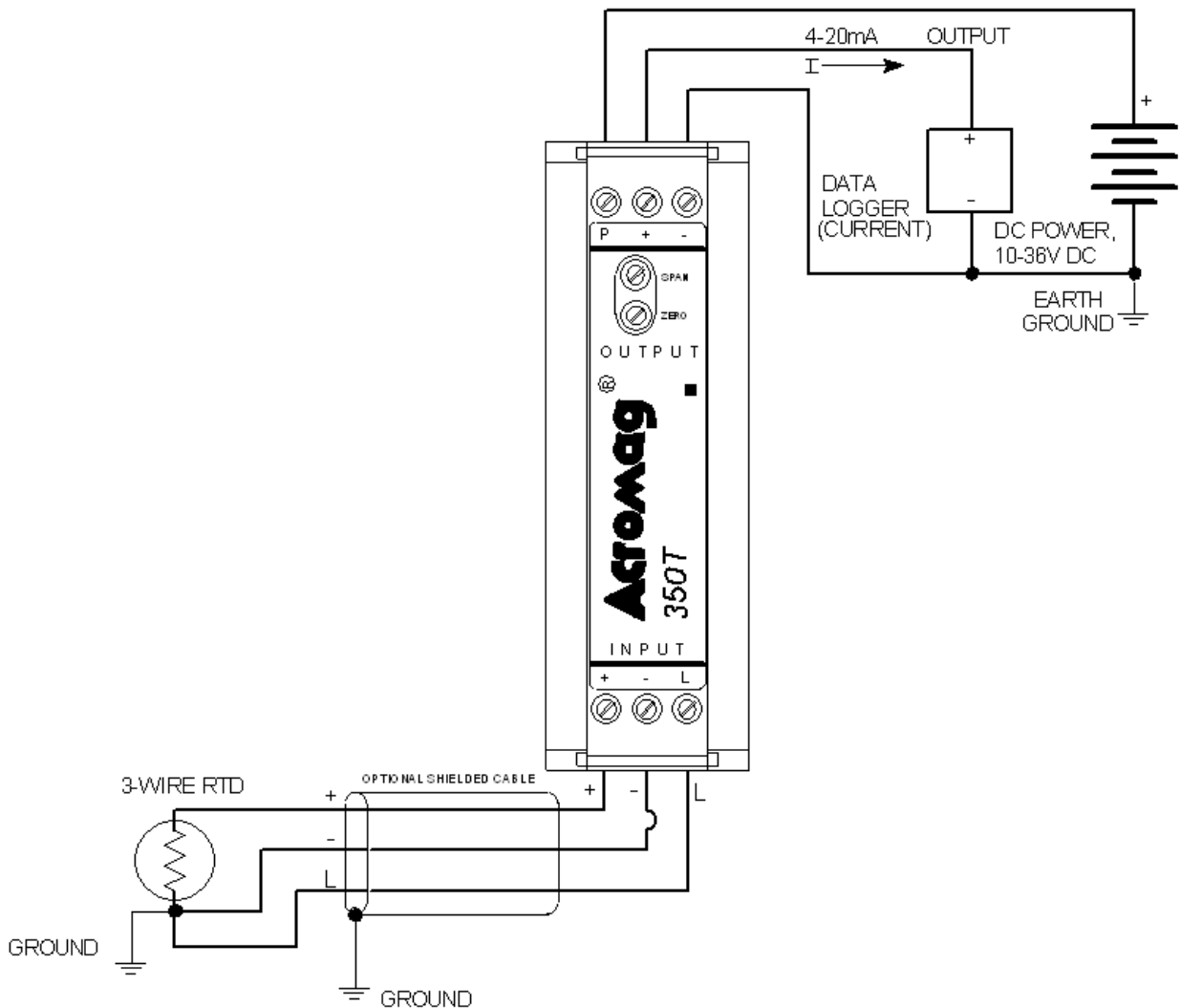


Figure 56 Wiring diagram for the W5228

Wiring description for the W5204

The input signal is 12mA. The positive lead on the current source will be connected to “IN +” on the W5204. The negative lead will be connected to the “24V+” terminal. The shielded wire around the negative and positive leads on the current source shall be equipment grounded. “IN -” is tied to RTN and instrument ground. The 24Vdc, 20A QUINT power supply assembly will be used to power the module. The positive power lead is connected to a 200mA high surge fuse, which is then connected to terminal labeled “DC+” on the W5204. The negative lead is connected to earth ground and the terminal labeled “DC-“. The terminal labeled “GND” is connected to earth ground. At the output the data logger will be connected between the outputs positive and negative terminals. The negative lead on the data logger is connected to the negative output terminal. The positive lead will be connected to the positive output terminal. Input impedance to the data logger must be below.

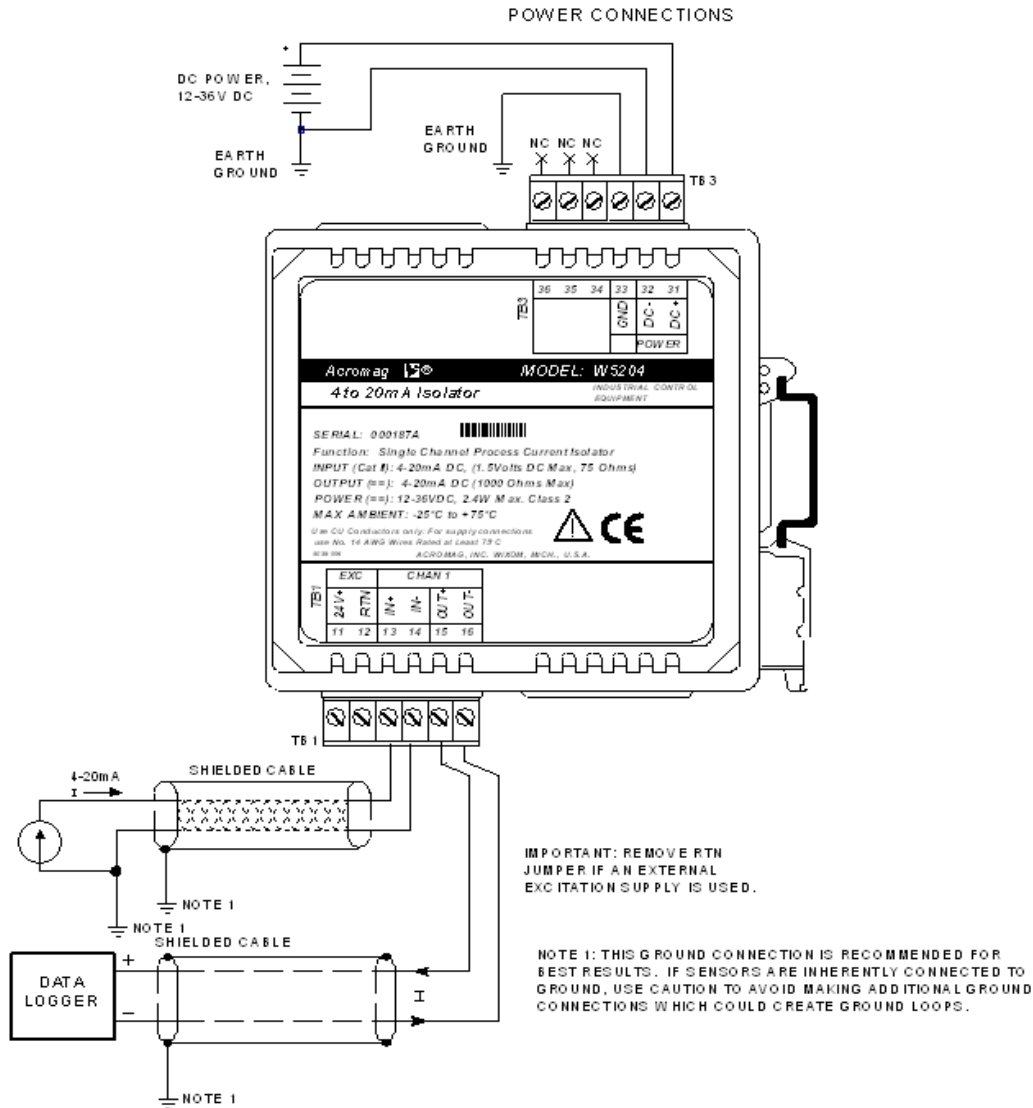


Figure 57 Wiring diagram for the W5204

Wiring description for the W5202

The input signal supplied is 12mA. The positive lead on the current source will be connected to “IN +” on the W5202. The negative lead will be connected to the “IN-” terminal and instrument ground. The shielded wire around the negative and positive leads on the current source shall be equipment grounded. The 24Vdc, 20A QUINT power supply assembly will be used to power the module. The positive lead on the voltage source is connected to a 200mA high tolerant fuse, which is then connected to the terminal labeled “DC+” on the W5202. The negative lead is connected to earth ground and the terminal labeled “DC-“. The Terminal labeled “GND” is connected to earth ground. At the output the data logger will be connected in series with the positive and negative terminals on the voltage setting. The positive lead on the data logger is connected to the positive output terminal. The negative lead will be connected to the negative output terminal.

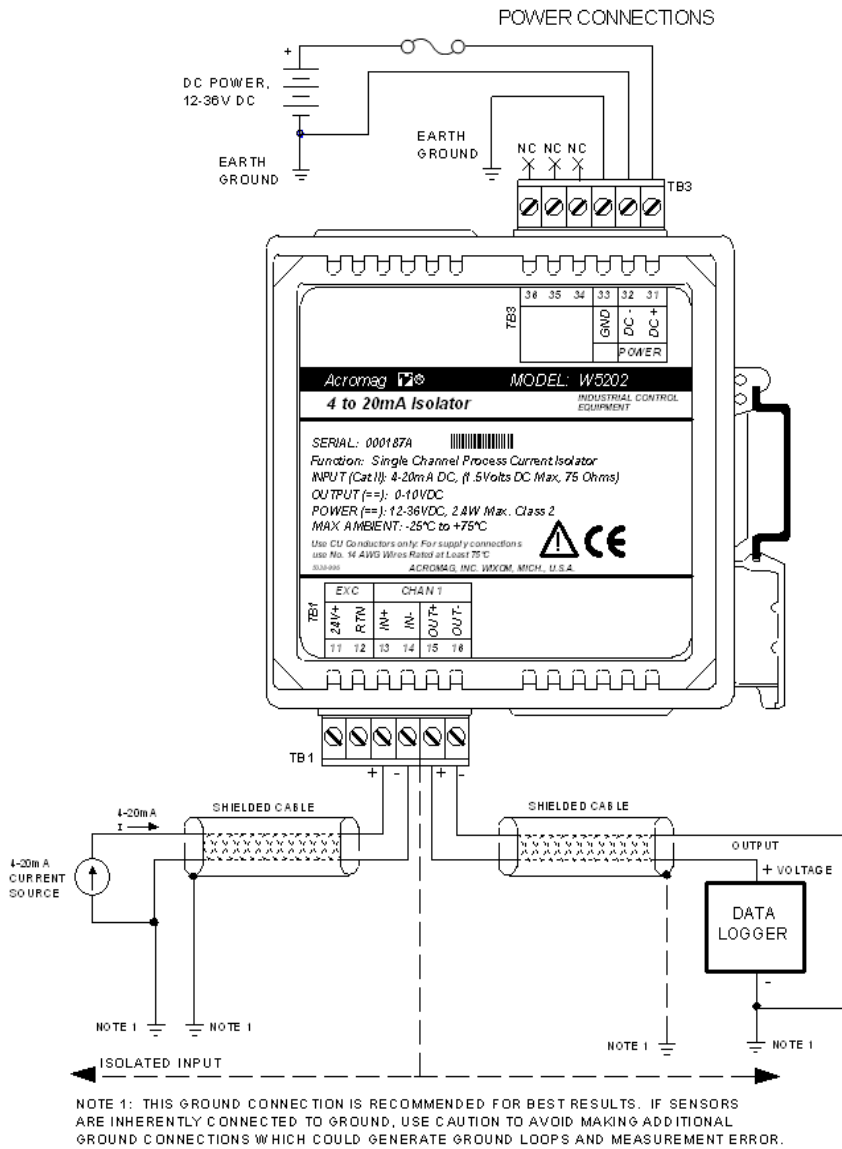


Figure 58 Wiring diagram for the W5202

Wiring description for the W5205

The input signal supplied is 12mA. The positive lead on the current source will be connected to “IN+” on the W5205. The negative lead will be connected to the “IN-” terminal and instrument ground. The shielded wire around the negative and positive leads on the current source shall be equipment grounded. The 24Vdc, 20A QUINT power supply assembly will be used to power the module. The positive power lead is connected to 200mA high tolerant fuse, which is then connected to the “OUT+” terminal on the W5205. The negative power lead and the negative lead on the data logger are connected to earth ground. The positive lead on the data logger is connected to the “OUT-” terminal.

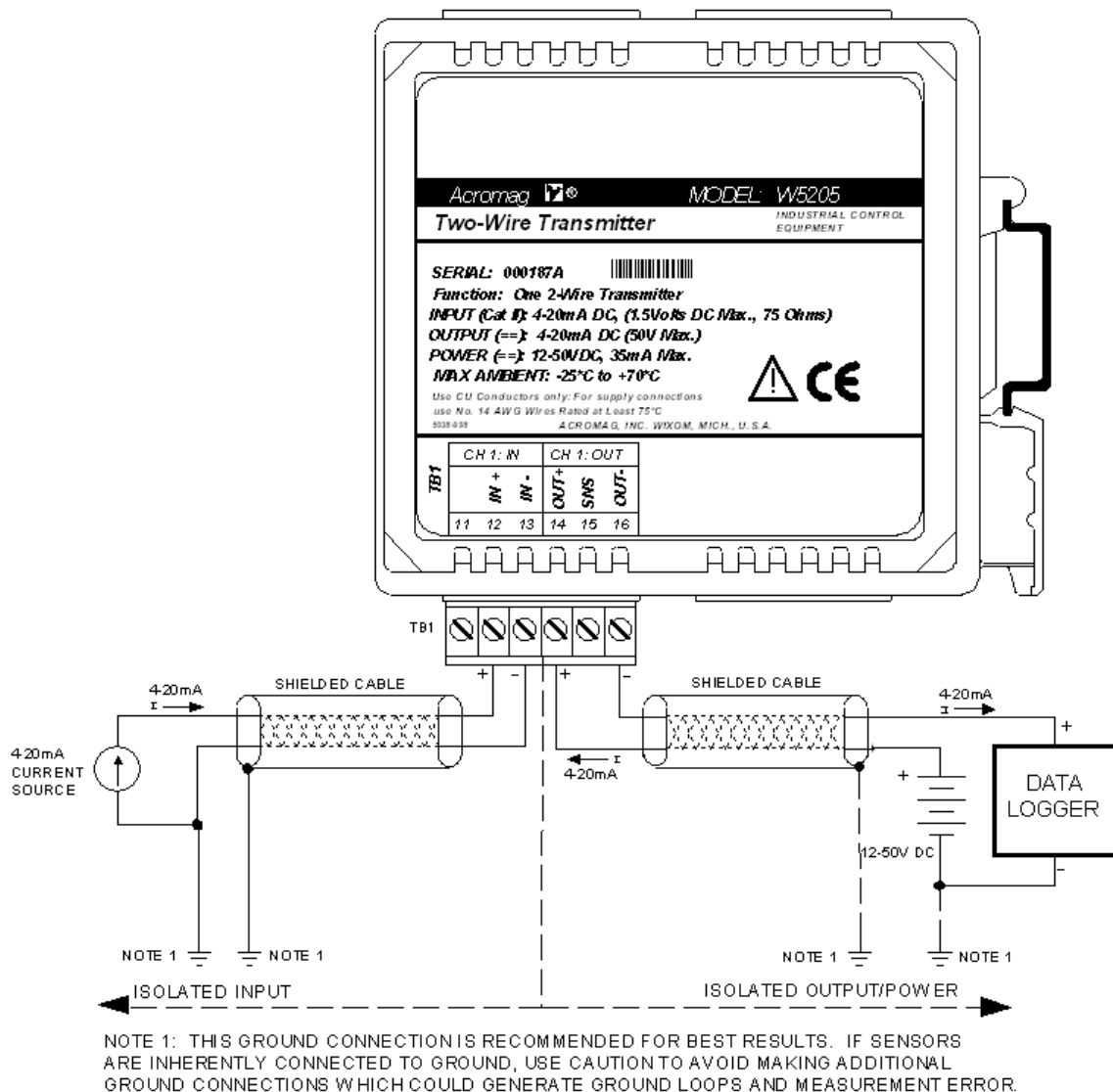


Figure 59 Wiring diagram for the W5205

Appendix C: Test Equipment

The test equipment will be used to monitor the Acromag Modules. All test equipment used during test must be in current calibration.

1. Qty. 1 Fluke 2640A/2645A NetDAQ Data Logger with accuracy of less than or equal to $\pm 0.025\%$.
2. Qty. 1 2620A-101 Current Shunt Resistors. Contains twelve (12) ten (10) $\pm 0.08\%$ ohm resistors.
3. Qty. 1 Power supply. The power supply is set to 24Vdc and capable of drawing 3A.
4. Qty. 2 200mA High surge-tolerant fuses (318P Series 3AG Fast-Acting axial Lead Fuses).
5. Qty. 2 fuse holders (155 series twist-lock in-line type fuse holders for 3AG-SFE)
6. Qty. 1 Variable dc Voltage source. Capable of reaching 6 volts. Used to drive the input to the W5206
7. Qty. 3 Thermocouple simulators. Capable of simulating Type E and K thermocouples.
8. Qty. 3mA calibrators (Current Source)
9. Qty. 5 Resistance Temperature Detector simulators (or precision Decade Box).
10. Qty. 1 Potentiometer, 2k Ω , Capable of adjustment to 1k Ω . Accuracy $\pm 1\%$.
11. Qty. 3 boxes of Terminal blocks. Type E thermocouple, Type K thermocouple, and regular terminal blocks.
12. Qty. 80 ft shielded twisted pair of Type E thermocouple wire.
13. Qty. 40 ft. shielded twisted pair of Type K thermocouple wire.
14. Qty. 880 ft, 3 Conductor Shielded Cable; one white, one black, and one red.
15. Qty. 3 Din Rail Kit 20.96" in length
16. Qty. 1 Digital Multimeter (DMM) for checking instruments with accuracy of equal to or less than $\pm 0.025\%$

Appendix D: Test Setup

1. Using a DMM, verify twelve (12) 2620A-101 Current Shunt Resistors are $10\Omega \pm 0.08\%$.
2. Place ten (10) 2620A-101 Current Shunt Resistors in shunt across the data loggers input terminals that require a current output reading.
3. Measure and set the $2k\Omega$ potentiometer to $\frac{1}{2}$ its maximum value prior to connecting to module.
4. Verify the potentiometer output is actually $\frac{1}{2}$ the measured maximum value at approximately $1.00785k\ \Omega (\pm 0.1\ %)$.
5. Set the RTD simulator input for module W5218 (RTD1; Input Cable 3) to Pt 100 ohm 385 at 26°C (110.12Ω).
6. Using a DMM, verify the RTD simulator input for module W5218 is 110.12Ω .
7. Set the RTD simulator input for module W5221 (RTD2; Input Cable 4) to Pt 100 ohm 385 at 280°C (204.9Ω).
8. Using a DMM, verify the RTD simulator input for module W5221 is 204.9Ω .
9. Set the RTD simulator input for module W5224 (RTD3; Input Cable 5) to Pt 100 ohm 385 at 66°C (125.54Ω).
10. Using a DMM, verify the RTD simulator input for module W5224 is 125.54Ω .
11. Set the RTD simulator input for module W5227 (RTD4; Input Cable 6) to Pt 100 ohm 385 at 200°C (175.86Ω).
12. Using a DMM, verify the RTD simulator input for module W5227 is 175.86Ω .
13. Set the RTD simulator input for module W5228 (RTD5; Input Cable 7) to Pt 100 ohm 385 at 175°C (166.63Ω).
14. Using a DMM, verify the RTD simulator input for module W5228 is 166.63Ω .
15. Turn on the 24Vdc Power Supply Assembly.
16. Using a DMM, verify the 24Vdc output of the Power Supply Assembly.
17. Turn on 5Vdc voltage source and set to 5V.

18. Using a DMM, verify the voltage source output is 5Vdc ($\pm 0.01\%+3\text{mV}$)
19. Set the E type thermocouple simulator input for module W5207 (TC1) consistent with 50°C.
20. Using a thermocouple calibrator, verify the thermocouple simulator input to module W5207 is 3.685mVDC.
21. Set the K type thermocouple simulator input for module W5214 (TC2) consistent with 100°C.
22. Using a thermocouple calibrator, verify the thermocouple simulator input to module W5214 is 4.509mVDC.
23. Set the E type thermocouple simulator input for module W5229 (TC3) consistent with 30°C.
24. Using a thermocouple calibrator, verify the thermocouple simulator input to module W5229 is 2.420mVDC.
25. Set the current source to “on”.
26. Using a DMM, verify the current source is supplying 12mA ($\pm 0.01\%+2$ counts).
27. Turn on the data logger.
28. Make sure the inputs are on the correct setting (Voltage/Current).
29. Wire up the circuit according to pervious section.
30. With everything powered up and connected correctly wait a half an hour before beginning initial testing.
31. Test the modules and recorded in Table 10.1-1 before EMI testing.
32. Begin EMI testing; Re-test the modules and record in Table 10.1-2.
33. Shortly after EMI testing, Re-test the modules and record in Table 10.1-3.
34. Repeat steps 2, 4, 6, 8, 10, 12, 14, 16, 18, 20, 22, and 24. Record in Table 10.1-3.

Note:

- 1 The test equipment readings should only vary within there accuracies.

- 2 To obtain the necessary current readings take the voltage that results and divide it by ten (10)

Appendix E: Expected Outputs with Tolerances

I/O Table of Acromag Modules (After Setup and Testing)

Data Logger Channel/ Westinghouse part number:	Manufacturer's part number:	Input	Output	Module Type	Input Cable	Output Cable
1.W5206	250T-V2-DIN-NCR-C	5Vdc	11.8912-12.1088mA	Voltage to Current Converter	Cable 1	Cable 11
2.W5207	350T-EL00-Y-DIN-NCR-C	50°C	11.7440-12.2560mA	TC (Type E input) to Current Converter	TC1	Cable 12
3.W5214	350T-KL00-Y-DIN-NCR-C	100°C	11.8240-12.1760mA	TC (Type K input) to Current Converter	TC2	Cable 13
4.W5229	350T-TC3-Y-DIN-NCR-C	30°C	13.016-13.892mA	TC (Type E input) to Current Converter	TC3	Cable 14
5.W5216	350T-P-Y-DIN-NCR	Max / 2 Approx. 1.00785k Ω	11.8912-12.1088mA	Potentiometer/Slide wire (input) to Current Converter	Cable 2	Cable 15
6.W5218	350T-RBP1-Y-DIN-NCR-C	26°C (110.12 Ω)	14.2672-14.5328mA	RTD (input) to Current Converter	Cable 3	Cable 16
7.W5221	Special 350T-RBP1-V0-DIN-NCR-C	280°C (204.90 Ω)	4.94-5.06Vdc	RTD (input) to Voltage Converter	Cable 4	Cable 17
12.W5224	350T-RBP2-Y-DIN-NCR-C	66°C (125.54 Ω)	11.8912-12.1088mA	RTD (input) to Current Converter	Cable 5	Cable 18
8.W5227	350T-RBP3-V0-DIN-NCR-C	200°C (175.86 Ω)	4.94-5.06Vdc	RTD (input) to Voltage Converter	Cable 6	Cable 19
13.W5228	350T-RBP3-Y-DIN-NCR-C	175°C (166.63 Ω)	11.8912-12.1088mA	RTD (input) to Current Converter	Cable 7	Cable 20
14.W5204	631T-0500	12mA	11.8192-12.1808mA	Current to Current Isolator	Cable 8	Cable 21
15.W5202	Special 631T-0500 (W5202)	12mA	4.895-5.105Vdc	Current to Voltage Converter	Cable 9	Cable 22
16.W5205	651T-0600	12mA	11.8112-12.1888mA	Current to Current Isolator	Cable 10	Cable 23

Note:

1. TC = Thermocouple
2. RTD = Resistance Temperature Detector

Appendix F: Ideal Expected Outputs

W5206 Ideal expected output

The output with accepted tolerances is given in Table 9.2-1. The Acromag W5206 module generates a current output signal (See Equation 1 below for ideal output calculation).

$$\begin{aligned}
 \text{Ideal Output} &= \left[\left(\frac{\text{Output Span}}{\text{Input Span}} \right) \times (\text{Actual Input} - \text{Input Zero}) + \text{Output Zero Offset} \right] \pm \\
 &\left[\text{Output span} \times \left(\frac{(\text{Combined Uncertainty} + \text{RFI Resistance} + \text{Resistor Uncertainty})}{100} \right) \right] \\
 \text{Ideal Output} &= \left[\left(\frac{16 \text{ mA}}{10 \text{ V}} \right) \times (5 \text{ V} - 0 \text{ V}) + 4 \text{ mA} \right] \pm \left[16 \text{ mA} \times \left(\frac{0.1\% + 0.5\% + 0.08\%}{100} \right) \right] = 12 \text{ mA} \pm 0.1088 \text{ mA}
 \end{aligned}$$

Equation 1: Output Calculation for the W5206 Module

W5207 Ideal expected output

The output with accepted tolerances is given in Table 9.2-1. The Acromag W5207 module generates a current output signal (See Equation 2 below for ideal output calculation).

$$\begin{aligned}
 \text{Ideal Output} &= \left[\left(\frac{\text{Output Span}}{\text{Input Span}} \right) \times (\text{Actual Input} - \text{Input Zero}) + \text{Output Zero Offset} \right] \pm \\
 &\left[\text{Output span} \times \left(\frac{(\text{Combined Uncertainty} + \text{RFI Resistance} + \text{Resistor Uncertainty})}{100} \right) \right] \\
 \text{Ideal Output} &= \left[\left(\frac{50^\circ \text{C}}{100^\circ \text{C}} \right) \times (16 \text{ mA}) + 4 \text{ mA} \right] \pm \left[16 \text{ mA} \times \left(\frac{1.02\% + 0.5\% + 0.08\%}{100} \right) \right] = 12 \text{ mA} \pm 0.2560 \text{ mA}
 \end{aligned}$$

Equation 2: Output Calculation for the W5207 Module

W5214 Ideal expected output

The output with accepted tolerances is given in Table 9.2-1. The Acromag W5214 module generates a current output signal (See Equation 3 below for ideal output calculation).

$$\begin{aligned} \text{Ideal Output} &= \left[\left(\frac{\text{Output Span}}{\text{Input Span}} \right) \times (\text{Actual Input} - \text{Input Zero}) + \text{Output Zero Offset} \right] \pm \\ &\left[\text{Output span} \times \left(\frac{(\text{Combined Uncertainty} + \text{RFI Resistance} + \text{Resistor Uncertainty})}{100} \right) \right] \\ \text{Ideal Output} &= \left[\left(\frac{16 \text{ mA}}{200^\circ\text{C}} \right) \times (100^\circ\text{C} - 0^\circ\text{C}) + 4 \text{ mA} \right] \pm \left[16 \text{ mA} \times \left(\frac{0.52\% + 0.5\% + 0.08\%}{100} \right) \right] = 12 \text{ mA} \pm 0.1760 \text{ mA} \end{aligned}$$

Equation 3: Output Calculation for the W5214 Module

W5229 Ideal expected output

The output with accepted tolerances is given in Table 9.2-1. The Acromag W5229 module generates a current output signal (See Equation 4 below for ideal output calculation).

$$\begin{aligned} \text{Ideal Output} &= \left[\left(\frac{\text{Output Span}}{\text{Input Span}} \right) \times (\text{Actual Input} - \text{Input Zero}) + \text{Output Zero Offset} \right] \pm \\ &\left[\text{Output span} \times \left(\frac{(\text{Combined Uncertainty} + \text{RFI Resistance} + \text{Resistor Uncertainty})}{100} \right) \right] \\ \text{Ideal Output} &= \left[\left(\frac{16 \text{ mA}}{3.047 \text{ mV}} \right) \times (1.801 \text{ mV} - 0 \text{ mV}) + 4 \text{ mA} \right] \pm \left[16 \text{ mA} \times \left(\frac{2.16\% + 0.5\% + 0.08\%}{100} \right) \right] = 13.454 \text{ mA} \pm 0.4384 \text{ mA} \end{aligned}$$

Equation 4: Output Calculation for the W5229 Module

W5216 Ideal expected output

The output with accepted tolerances is given in Table 9.2-1 The Acromag W5216 module generates a current output signal (See Equation 5 below for ideal output calculation).

$$\begin{aligned} \text{Ideal Output} &= \left[\left(\frac{\text{Output Span}}{\text{Input Span}} \right) \times (\text{Actual Input} - \text{Input Zero}) + \text{Output Zero Offset} \right] \pm \\ &\left[\text{Output span} \times \left(\frac{(\text{Combined Uncertainty} + \text{RFI Resistance} + \text{Resistor Uncertainty})}{100} \right) \right] \\ \text{Ideal Output} &= \left[\left(\frac{16\text{mA}}{2\text{K}} \right) \times (1\text{K} - 0\text{K}) + 4\text{mA} \right] \pm \left[16\text{mA} \times \left(\frac{0.1\% + 0.5\% + 0.08\%}{100} \right) \right] = 12\text{ mA} \pm 0.1088\text{mA} \end{aligned}$$

Equation 5: Output Calculation for the W5216 Module

W5218 Ideal expected output

The output with accepted tolerances is given in Table 9.2-1 The Acromag W5218 module generates a current output signal (See Equation 6 below for ideal output calculation).

$$\begin{aligned} \text{Ideal Output} &= \left[\left(\frac{\text{Output Span}}{\text{Input Span}} \right) \times (\text{Actual Input} - \text{Input Zero}) + \text{Output Zero Offset} \right] \pm \\ &\left[\text{Output span} \times \left(\frac{(\text{Combined Uncertainty} + \text{RFI Resistance} + \text{Resistor Uncertainty})}{100} \right) \right] \\ \text{Ideal Output} &= \left[\left(\frac{16\text{mA}}{40^\circ\text{C}} \right) \times (26^\circ\text{C} - 0^\circ\text{C}) + 4\text{mA} \right] \pm \left[16\text{mA} \times \left(\frac{0.25\% + 0.5\% + 0.08\%}{100} \right) \right] = 14.4\text{ mA} \pm 0.1328\text{mA} \end{aligned}$$

Equation 6: Output Calculation for the W5218 Module

W5221 Ideal expected output

The output with accepted tolerances is given in Table 9.2-1 The Acromag W5221 module generates a voltage output signal (See Equation 7 below for ideal output calculation).

$$\begin{aligned} \text{Ideal Output} &= \left[\left(\frac{\text{Output Span}}{\text{Input Span}} \right) \times (\text{Actual Input} - \text{Input Zero}) + \text{Output Zero Offset} \right] \pm \\ &\quad \left[\text{Output span} \times \left(\frac{(\text{Combined Uncertainty} + \text{RFI Resistance})}{100} \right) \right] \\ \text{Ideal Output} &= \left[\left(\frac{10 \text{ V}}{100^\circ\text{C}} \right) \times (280^\circ\text{C} - 230^\circ\text{C}) \right] \pm \left[10\text{V} \times \left(\frac{0.1\% + 0.5\%}{100} \right) \right] = 5\text{V} \pm 0.06\text{V} \end{aligned}$$

Equation 7: Output Calculation for the W5221 Module

W5224 Ideal expected output

The output with accepted tolerances is given in Table 9.2-1. The Acromag W5224 module generates a voltage output signal (See Equation 8 below for ideal output calculation).

$$\begin{aligned} \text{Ideal Output} &= \left[\left(\frac{\text{Output Span}}{\text{Input Span}} \right) \times (\text{Actual Input} - \text{Input Zero}) + \text{Output Zero Offset} \right] \pm \\ &\quad \left[\text{Output span} \times \left(\frac{(\text{Combined Uncertainty} + \text{RFI Resistance} + \text{Resistor Uncertainty})}{100} \right) \right] \\ \text{Ideal Output} &= \left[\left(\frac{16 \text{ mA}}{168^\circ\text{C}} \right) \times (66^\circ\text{C} + 18^\circ\text{C}) + 4 \text{ mA} \right] \pm \left[16\text{mA} \times \left(\frac{0.1\% + 0.5\% + 0.08\%}{100} \right) \right] = 12 \text{ mA} \pm 0.1088\text{mA} \end{aligned}$$

Equation 8: Output Calculation for the W5224 Module

W5227 Ideal expected output

The output with accepted tolerances is given in Table 9.2-1. The Acromag W5227 module generates a voltage output signal (See Equation 9 below for ideal output calculation)

$$\begin{aligned} \text{Ideal Output} &= \left[\left(\frac{\text{Output Span}}{\text{Input Span}} \right) \times (\text{Actual Input} - \text{Input Zero}) + \text{Output Zero Offset} \right] \pm \\ &\quad \left[\text{Output span} \times \left(\frac{(\text{Combined Uncertainty} + \text{RFI Resistance})}{100} \right) \right] \\ \text{Ideal Output} &= \left[\left(\frac{10 \text{ V}}{400^\circ\text{C}} \right) \times (200^\circ\text{C} - 0^\circ\text{C}) \right] \pm \left[10\text{V} \times \left(\frac{0.1\% + 0.5\%}{100} \right) \right] = 5\text{V} \pm 0.06\text{V} \end{aligned}$$

Equation 9: Output Calculation for the W5227 Module

W5228 Ideal expected output

The output with accepted tolerances is given in Table 9.2-1. The Acromag W5228 module generates a current output signal (See Equation 10 below for ideal output calculation).

$$\begin{aligned} \text{Ideal Output} &= \left[\left(\frac{\text{Output Span}}{\text{Input Span}} \right) \times (\text{Actual Input} - \text{Input Zero}) + \text{Output Zero Offset} \right] \pm \\ &\quad \left[\text{Output span} \times \left(\frac{(\text{Combined Uncertainty} + \text{RFI Resistance} + \text{Resistor Uncertainty})}{100} \right) \right] \\ \text{Ideal Output} &= \left[\left(\frac{16 \text{ mA}}{350^\circ\text{C}} \right) \times (175^\circ\text{C} - 0^\circ\text{C}) + 4 \text{ mA} \right] \pm \left[16\text{mA} \times \left(\frac{0.1\% + 0.5\% + 0.08\%}{100} \right) \right] = 12 \text{ mA} \pm 0.1088\text{mA} \end{aligned}$$

Equation 10: Output Calculation for the W5228 Module

W5204 Ideal expected output

The output with accepted tolerances is given in Table 9.2-1. The Acromag W5204 module generates a current output signal (See Equation 11 below for ideal output calculation).

$$\begin{aligned} \text{Ideal Output} &= \left[\left(\frac{\text{Output Span}}{\text{Input Span}} \right) \times (\text{Actual Input} - \text{Input Zero}) + \text{Output Zero Offset} \right] \pm \\ &\left[\text{Output span} \times \left(\frac{(\text{Combined Uncertainty} + \text{RFI Resistance} + \text{Resistor Uncertainty})}{100} \right) \right] \\ \text{Ideal Output} &= \left[\left(\frac{16 \text{ mA}}{16 \text{ mA}} \right) \times (12 \text{ mA} - 4 \text{ mA}) + 4 \text{ mA} \right] \pm \left[16 \text{ mA} \times \left(\frac{0.05\% + 1\% + 0.08\%}{100} \right) \right] = 12 \text{ mA} \pm 0.1808 \text{ mA} \end{aligned}$$

Equation 11: Output Calculation for the W5204 Module

W5202 Ideal expected output

The output with accepted tolerances is given in Table 9.2-1. The Acromag W5202 module generates a voltage output signal (See Equation 12 below for ideal output calculation).

$$\begin{aligned} \text{Ideal Output} &= \left[\left(\frac{\text{Output Span}}{\text{Input Span}} \right) \times (\text{Actual Input} - \text{Input Zero}) + \text{Output Zero Offset} \right] \pm \\ &\left[\text{Output span} \times \left(\frac{(\text{Combined Uncertainty} + \text{RFI Resistance})}{100} \right) \right] \\ \text{Ideal Output} &= \left[\left(\frac{10 \text{ V}}{16 \text{ mA}} \right) \times (12 \text{ mA} - 4 \text{ mA}) \right] \pm \left[10 \text{ V} \times \left(\frac{0.05\% + 1\%}{100} \right) \right] = 5 \text{ V} \pm 0.105 \text{ V} \end{aligned}$$

Equation 12: Output Calculation for the W5202 Module

W5205 Ideal expected output

The output with accepted tolerances is given in Table 9.2-1. The Acromag W5205 module generates a current output signal (See Equation 13 below for ideal output calculation).

$$\begin{aligned} \text{Ideal Output} &= \left[\left(\frac{\text{Output Span}}{\text{Input Span}} \right) \times (\text{Actual Input} - \text{Input Zero}) + \text{Output Zero Offset} \right] \pm \\ &\left[\text{Output span} \times \left(\frac{(\text{Combined Uncertainty} + \text{RFI Resistance} + \text{Resistor Uncertainty})}{100} \right) \right] \\ \text{Ideal Output} &= \left[\left(\frac{16\text{mA}}{16\text{mA}} \right) \times (12\text{ mA} - 4\text{mA}) + 4\text{mA} \right] \pm \left[16\text{mA} \times \left(\frac{0.1\% + 1\% + 0.08\%}{100} \right) \right] = 12\text{ mA} \pm 0.1888\text{mA} \end{aligned}$$

Equation 13: Output Calculation for the W5205 Module